Synthesis of Multi-dimensional Organic Nano-conductors for the Enhancement of Thermal, Electrical, and Mechanical Properties of Composites

by

James William Smith II

A thesis submitted to the Graduate Faculty of
Auburn University
in partial fulfillment of the
requirements for the Degree of
Master of Science

Auburn, Alabama
May 4, 2014

Keywords: carbon fiber, conducting polymers, nanofiller, epoxy, reinforced composites

Approved by

Xinyu Zhang, Chair, Associate Professor of Polymer and Fiber Engineering
Sabit Adanur, Professor of Polymer and Fiber Engineering
Hareesh Tippur, McWane Professor of Mechanical Engineering

Abstract

For years, composite materials have attracted significant attention toward the improvement of their mechanical, electrical, and thermal properties. In more recent studies, carbon based fillers, such as carbon fibers, have received a large amount of interest because of their strong mechanical and thermal properties. Researchers have begun using nano-sized fillers due to the large surface areas and high aspect ratios. One of the widely used fillers is carbon nanotubes (CNTs). Typically synthesized by the Chemical Vapor Deposition method, the rate of production tends to be slower and more expensive than our recently developed microwave-assisted synthesis, using conducting polymer and metallocene as precursors.

This Master's thesis suggests the synthesis of inexpensive, multi-dimensional nano-conductors through microwave assisted carbonization using two different carbon based substrates, milled carbon fiber and carbon fiber fabric. These one dimensional substrates were subjected to the introduction of metallocene catalysts and microwave irradiation to synthesize carbon nanostructures on the surface of the substrates to ultimately produce a three dimensional filler that could enhance an epoxy composite mechanically, thermally, and electrically.

The synthesized fillers were characterized specifically for their surface properties using Scanning Electron Microscopy, thermally using Thermogravimetric Analysis and electrically using two and four probe electrical conductivity measurements. Once the best overall filler was chosen, based on these results, the synthesized material was incorporated into an epoxy composite and further characterization was completed to determine the fillers effects on the composite material.

Acknowledgments

The author would like to express his thanks to his advisor and mentor, Dr. Xinyu Zhang, for his guidance, advice, and time contributed to the project and academic development of the author. The author would also like to thank Dr. Hareesh Tippur and the rest of the committee members for their suggestions and contributions toward the project.

The author owes a special thank you to another mentor and previous research group member, Dr. Zhen Liu, for his contributions, guidance, and beloved advice. The author would also like to thank research group members, Selcuk Poyraz and Xialaong Wang, for their efforts toward the completion of this project. Also, the author recognizes, Clifford Jones and Adam Wypyski, two undergraduate students for their hard work and sincere efforts.

A special thank you goes out to the Department of Polymer and Fiber Engineering for creating an environment in which to grow both as a student and researcher. The author would like to thank all of the faculty and staff for their support and commitment to the development and teaching of students.

The author would like to thank his wife, Katelyn, for her love and continued support toward the completion of his academic goals. The author would also like to thank his parents, Jim and Barbara, for their sincere love and support.

Finally, the author would like to express his utmost thanks and appreciation to the National Science Foundation and NASA for their financial contributions under grants CMMI-1100700 and NNX13AB80A, respectively.

Table of Contents

List of Tables

List of Figures

List of Abbreviations

APS	Ammonium Persulfate
APT	Acetone Pretreatment
CF	Carbon Fiber
CFF	Carbon Fiber Fabric
CNT	Carbon Nanotube
CNTs	Carbon Nanotubes
CVD	Chemical Vapor Deposition
DI	Deionized Water
DMA	Dynamic Mechanical Analysis
DSC	Differential Scanning Calorimetry
E’	Storage Modulus
E”	Loss Modulus
Epon	Epon 862 Resin
EtOH	Ethanol
Exo	Exothermic
HCl	Hydrochloric Acid
MCF	Milled Carbon Fiber
MIC	Microwave Initiated Carbonization

mL	Milliliter
MPT	Microwave Pretreatment
MW	Microwaved
MWNT	Multiwall Carbon Nanotube
n	Crosslink Density
PPy	Polypyrrole
PPyG	Polypyrrole Granules
PPyF	Polypyrrole Fibers
SEM	Scanning Electron Microscopy
SWNT	Single Wall Carbon Nanotube
T_g	Glass Transition Temperature
TGA	Thermogravimetric Analysis
THF	Tetrahyrdrofuran

CHAPTER 1

LITERATURE REVIEW

1.1 Introduction

In recent years, extensive research has been done on composite materials as they offer improved properties such as high strength, electrical conductivity, and thermal conductivity at a fraction of the weight of common materials. Their fatigue resistance is often greater than that of a comparable metal structure, and these composites also reduce the life cycle costs due to reduced maintenance. Simple composite materials, although strong, are not applicable in every situation.

In order to improve the properties of simple composite materials, fillers are incorporated to maximize the mechanical, electrical, and thermal properties. These fillers can range from being long continuous fibers to nano-sized particles. More recently, a lot of research has been conducted on the nano-sized fillers. The reason behind using nano-sized fillers results from the ability to add filler without adding significant weight and the large surface area on the particles. These nanofillers can also add significant improvements in the mechanical, electrical, and thermal properties. The increase in these properties opens up the opportunity for these composites to be used in more advanced and technical applications.

An extensive amount of research has been conducted with Carbon nanotubes (CNTs) due to their unique mechanical, electrical, and thermal properties.

1.2 Composite Materials

According to Merriam-Webster, a composite is defined as being made up of distinct parts. These parts are normally different materials with different physical and chemical properties. There are typically two components in a composite material, the matrix phase and the dispersed phase. The matrix phase is the primary phase, and is normally the more ductile phase of the two. It contains the dispersed phase and shares any applied load with it. The dispersed phase is usually stronger, though not always, than the more ductile matrix and provides reinforcement tailored to the application[1].

There are numerous advantages of composites over non-composites that include: lighter weight, the ability to tailor the lay-up for optimum strength and stiffness, improved fatigue life, corrosion resistance, and with good design practice, reduced assembly costs due to fewer detail parts and fasteners[2]. Engineered composite materials typically fall under one of three different categories: ceramic, metal, and polymer composites[3]. An example of each can be seen below in Figure 1.

Figure 1 (from left to right): Ceramic Composite Thrustcells[4], High Performance Metal Composite Brake Pad [5], and a Polymer Composite Manhole Cover [6]

1.2.1 Composite Structure

There are three main composite structures within any of the three composite categories, these include: Particulate, Fibrous, and Laminate composites**.** All three are a version of reinforcing the matrix whether it is a ceramic, metal, or polymer matrix. In Figure 2, the three different composite structures are depicted. Particulate composites are reinforced by one or more different particulate materials. Fibrous composites are constructed of short fibers and the matrix in order to provide extra strength and stability to the composite. Finally, laminate composites are fabricated of many stacked layers of continuous fiber and then infused with the desired matrix.

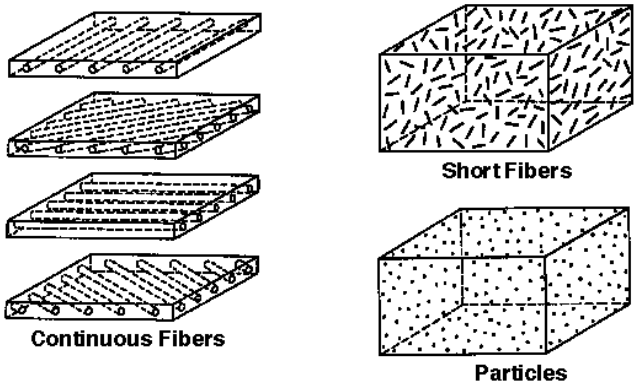

Figure 2: Schematic of Different Composite Structures[7]

1.2.1.1 Particulate Composites

Particulate Composites are made from a matrix with suspended/dispersed reinforcing particles. Some common particles shapes can be seen in Figure 3. Particulate composites typically fall under two categories: composites with random orientation of particles and composites with preferred orientation of particles. Random orientation pertains to embedded particles that have no ordered spacing or direction, i.e. random. Preferred orientation is just the opposite. Particles will have a noticeable trend whether it is exact spacing or alignment. Random orientation and preferred orientation can be achieved with any shape of particle filler, yet plate-like or acicular particles are more commonly used when preferred orientation is desired.

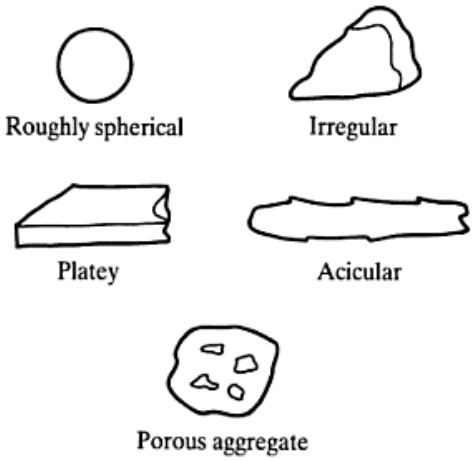

Figure 3: Particle Types found in Common Fillers

Particulate composites are useful in some cases, but there are limitations. The largest drawback is the way particles disperse into the matrix and how much energy is needed to do so. In Figure 4, an idealized view of how particle size and dispersion energy relate. Large particles or agglomerates only need a small amount of energy applied to disperse this particle size. The smaller the size of the particles along with how closely they are arranged determines how easily that can be dispersed. The small particles or filler like Carbon nanotubes (CNTs) tend to agglomerate and require large amount of energy to disperse; this is consistent with Figure 4.

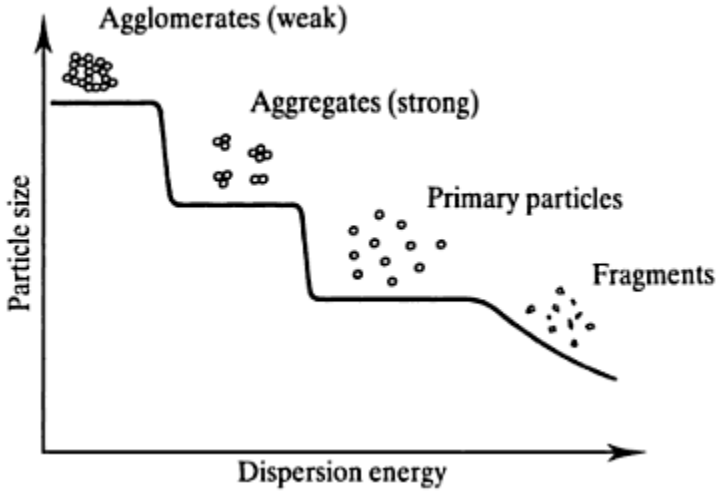

Figure 4: Idealized view of how particle fillers disperse

1.2.1.2 Fibrous Composites

In fibrous composites, the composite receives a unique blend of a ductile response of the polymer matrix and the brittle response of the fiber filler. The strength and stiffness along the length of the fiber is an average of both the fiber and polymeric matrix, thus improving the properties of plain matrix. Some fibrous filler include: Glass, Carbon, and Kevlar fibers among others. The toughness of these composites tends to be higher than either the fiber or the matrix. The toughness is higher because cracks are unable to easily propagate. They become trapped within the matrix, and it develops into a maze for the crack to propagate and cause failure. Toughness is also enhanced during fiber pull-out. Pulling out fibers requires work which correlates to increased toughness.

A major advantage to fibrous composites is cost and time savings. Lay-up, which is required in laminate composites, can be very costly and time consuming. Adding short or chopped fibers eliminates the lay-up step, therefore saving money. Short fibers can actually being incorporated through injection molding as well, which make processing much easier[8].

1.2.1.3 Laminate Composites

Like previously stated, a laminate is, simply, layers of matrix saturated fabric constructed to obtain a set of ideal properties for a chosen application. These laminates can offer enhanced mechanical properties compared to more conventional materials, such as metal. This can be seen below in Figure 5. The graph illustrates a composite material's ability to resist deformation and fatigue, which are both important factors in a structural application. These characteristics of a laminate can be further improved during the fabrication of the composite.

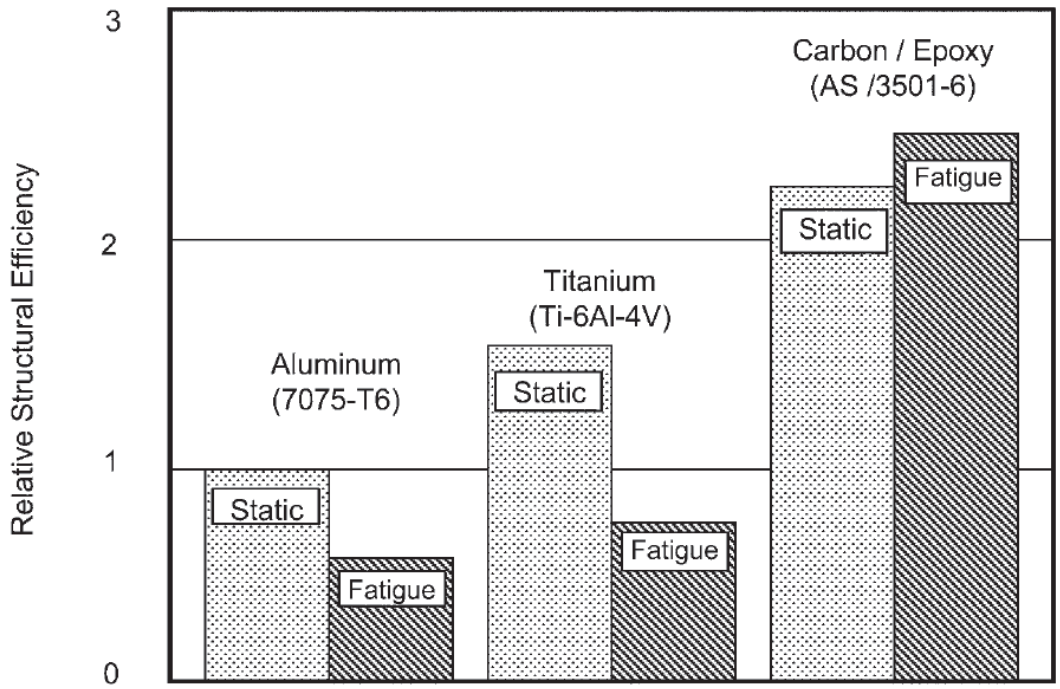

Figure 5: Structural Efficiency of Laminates vs. Metals[2]

There are many important factors to consider when fabricating a laminate composite. The main two are which fabrics and matrix will be used. The fabric will provide much of the strength and support for the final composite, while the matrix bonds the layers and can provide chemical resistance along with other critical properties. Like other composite structures, the final composite can be tailored based on what materials are used and their alignment. For example, multiple fabric materials can be used in order to get specific desired properties. This is called a hybrid laminate. The challenge with using multiple fabric varieties is that it becomes more difficult to find a matrix that will bond with different material layers. Alignment is also another important decision. By aligning the fabric layers in different orientations, like seen below in Figure 6, the composite can have strength in a multitude of directions instead of traditional longitudinal and lateral directions.

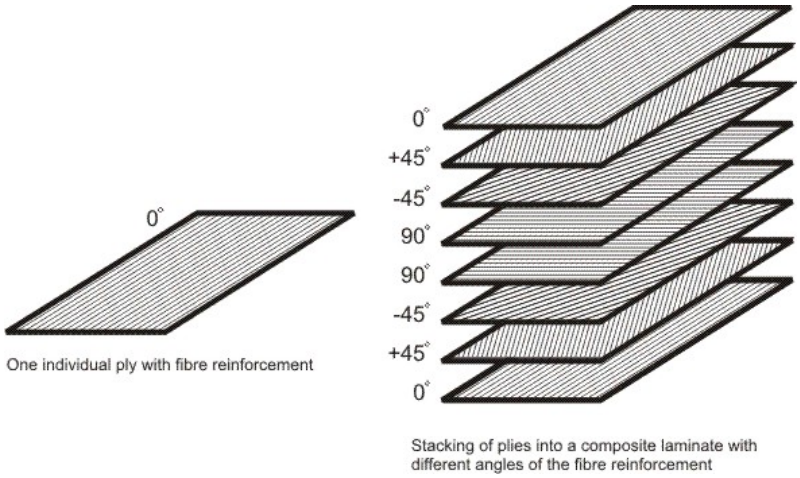

Figure 6: Ply Orientations for Laminate Composite[9]

1.2.2 Conventional Composite Applications

Composite usage typically spans over a large variety of applications. Composites are used in aerospace, transportation, marine, construction, and sporting good industries. Carbon fiber composites are used where high strength and stiffness along with lightweight are needed while fiber glass composites can be used in less demanding applications.

In the aerospace industry, low weight is extremely important for performance, fuel performance, and cargo carrying capability so composites are often used. Actually, composites make up approximately 20-40 percent of the airframe of an aircraft, which helps reduce weight by 15-25 percent.

The automotive industry also uses composites to reduce weight and increase performance, thus improving the fuel efficiency. Since cost is a major issue in commercial transportation, composites allow for lower weight and lower maintenance costs. Commercial transportation composites typically consist of fiberglass and polyurethane, while recreational vehicles use used glass fibers for durability and weight savings compared to conventional metals or alloys. High performance race cars normally consist of carbon fiber composite components since cost is not a major player in this category.

For marine applications, weight, buoyancy, and corrosion are major concerns. Composites play a large role in helping with corrosion as they don't corrode like metal or rot like wood. Composites are used on both the hulls and masts of the boats. For the hull, glass fiber and polyester or vinyl ester resins are used. The masts are commonly constructed from carbon fiber composites. Scuba gear is also included under composite use within the marine industry. Scuba tanks can be fabricated from fiberglass by filament winding. This allows for less weight and the ability to hold more air for divers. Naval ships have also incorporated using composites in their construction. The mast in modern day naval ships holds important radar and other equipment and in order to reduce weight have been fabricated from composite material as well.

In construction, there are several areas that consist of composite components. Road and bridges are one of the newer ventures within the construction field. Being that a lot of roads and bridges are corroded or in need of repair, composites are attractive because they offer a longer life span and less maintenance over that life. Fiberglass rebar is used to strengthen concrete, and large portions of shingling materials are constructed using glass fiber. With a reduction in mature trees available and the capability of creating stronger alternatives, light and power poles made from composite materials are becoming a more popular.

Composites in the sporting world have been around for quite some time. Tennis rackets, golf clubs, surfboards, and snowboards/skis are made from composite materials. Tennis rackets are typically made from fiber glass, while golf club shafts can be fabricated from carbon fiber. The benefit of using composites in the sporting good industry is that the products become lighter, and stronger, therefore allowing for new sporting heights to be achieved.

1.3 Epoxy Composites

Due to their high-adhesion, low-weight, and good chemical resistance, epoxy-based composite materials are being increasingly used as structural components in the aerospace, military automobile, and sports equipment industries. However, the relatively weak mechanical properties of epoxy have prevented its application in the components that demand high mechanical strength and stability.

1.4 Potential Epoxy Composite Fillers

Nanofillers have started receiving attention with the hopes of strengthening epoxy matrices. There have been several researchers that have added carbon based material into an epoxy matrix and had improved results. Carbon black, carbon fiber, and carbon nanotubes are some of those carbon based fillers. Montazeri et al showed that, when nanocomposites were produced by addition of 0.5 wt% MWNT, tensile strength and the Young's modulus of MWNT/epoxy increased. Zhou et al reported a 19.4% increase in Young's modulus with only 3 wt. % carbon nano fibers.

Another outlet for the improvement in epoxy composite materials is the electrical conductivity of these composites. Epoxy, itself tends to be an insulator. So by introducing fillers that electrically conductive, epoxy's conductivity can be enhanced.

1.4.1 Carbon Nanotubes

Carbon nanotubes (CNTs) date back further than Iijima in 1991. In the early 1950s, V. M. Lukyanovich and V. Radushkevich are credited with discovering carbon tubes, but due to lack of access to Soviet Press, much of the western world was unaware of the discovery. There were discoveries and advancements in carbon fibers/tubes between 1952-1991, yet the next major discovery was by Sumio Iijima in 1991. Iijima found carbon nanotubes in the soot of arc

discharge experiments. Also in 1991, Al Harrington and Tom Maganus discovered nanotubes in the chemical vapor deposition (CVD) process they were using. It is worth noting that the CVD process is still used to this day for the production of CNTs [10].

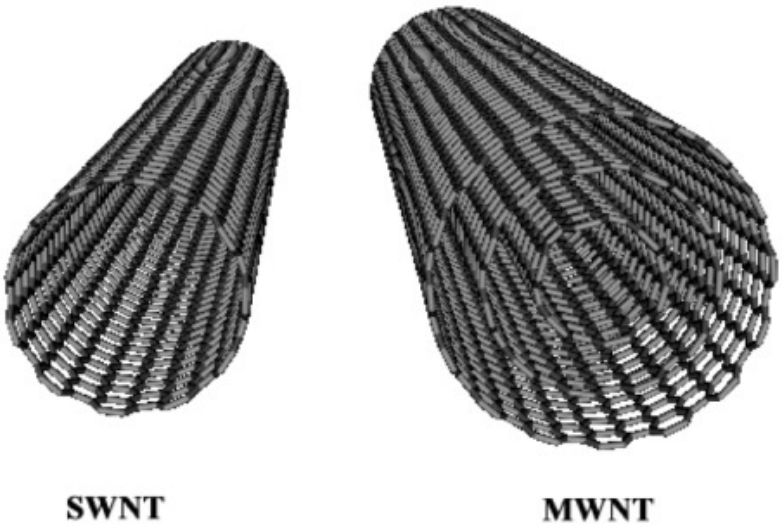

Figure 7: Structure of Single wall and Multi-wall Carbon Nanotubes[11]

Synthesizing of CNTs has a broad range of processes. Like previously stated, Iijima found CNTs in the soot from Arc discharge. Similar to arc discharge, plasma torching can be used. In plasma torching, a coil generates oscillating currents that create a thermal plasma. Carbon rich feedstocks are fed into the plasma and then cooled creating CNTs. Laser ablation has also been used to synthesize CNTs. In laser ablation, a pulsed laser vaporizes a graphite target inside of a high temperature reactor while maintaining an inert gas environment. As the reactor cools, nanotubes develop on the surface of the reactor and are later collected. One of them more common methods used for CNT production is CVD. In CVD, a substrate is used and decorated with metal catalyst particles. These particles act as growth sites for the CNTs. The decorated substrate is placed in a furnace and heated with a process gas and a feedstock gas that

are pumped in. The process gas maintains the environment while the feedstock gas provides more carbon sources for CNT growth.

A more recent CNT growth process is microwave assisted carbonization. In this process, a conductive substrate is used in combination with a metallocene catalyst and then subjected to microwave irradiation. The metallocene catalyst, Figure 8, typically consists of two cyclopentadienyl rings sandwiching a metal atom. Upon microwave irradiation, high temperatures cause the five member ring to dismember, and the carbon atoms rearrange themselves to for nano-sized carbon tubes.

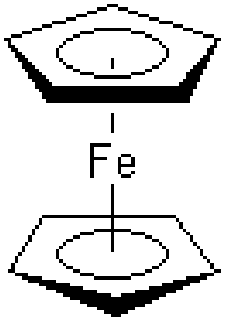

Figure 8: Chemical Structure of Ferrocene, the First Catergorized Metallocene[12]

The reason CNTs are so popular lend to their unique properties. Mechanically, CNTs have been considered the stiffest known fiber with a measured Young's modulus of up to 1.4 TPa. They are said to have an expected elongation-to-failure of 20-30% and when combined with their high stiffness, a tensile strength well above 100 GPa can be projected. For comparison, steel boasts a Young's modulus around 200 GPa and a tensile strength of 1-2 GPa [10].

When considering the electrical capabilities of CNTs, they can vary from semiconducting to metallic and are defined by two indices, n and m. If n-m is zero or a multiple of 3, the tubes tend to conduct electricity very well and fall in the metallic conductor category. All of the other n-m relate to a semi-conductor. Carbon nanotube ropes have been measured to have a resistivity

of 10^{-4} ohm-cm at room temperature, making them the most electrically-conductive fibers known[10].

CNTs are also known to be great thermal conductor along the length of the tube, and in the past had surpassed diamond's thermal conductivity levels. In 2002, CNTs had shown a thermal conductivity of approximately 3000 Watts per meter-degree Kelvin according to Dresselhaus, et al. Thermal stability is also an important characteristic that CNTs own.

These unique properties lead to current and potential applications of CNTs. Currently, CNTs are used in many structural composite applications such as wind turbine blades, marine vessels, bicycle components, and other sports related equipment. The reason behind these applications lends to CNTs being lightweight and incredibly strong. As far as potential applications go, the possibilities are practically endless. CNTs have been considered for more structural applications, electrical circuits/cables/wires, actuators, paper batteries, solar cells, and super capacitors. Some other potential applications include: radar aborption, medical, textile, speaker technology, and many others. The two largest hindrances of using CNTs are the cost and difficulty of synthesis and production. This is why many researchers are finding way to make synthesis cheaper and more effective or finding new fillers that are cheaper substitutes for CNTs.

1.4.2 Conducting Polymers

The discovery of conducting polymers dates back to the mid-1950s, yet it wasn't until the 1970s that a large discovery was made. In 1977, Hideki Shirakawa, Alan MacDiarmid, and Alan Heeger, seen in Figure 9, decided to expose high quality films of trans-polyacetylene to bromine vapor at room temperature and measure the conductivity of the film using a four point probe. This experiment yielded 10 million time increase in conductivity in just a few minutes. Prior to this major discovery, many researchers had only considered polymeric semi-conductors that

could be made conductive through major alterations in their chemical nature, like by pyrolysis or partial graphitization[13].

Figure 9 (from left to right): Hideki Shirakawa, Alan MacDiarmid, and Alan Heeger[14]

During that last few decades, conducting polymers have gathered great interest in both academia and industry by combining the electrical properties of semiconductors and metals with the advantages of conventional polymers such as easy and low cost of fabrication into the same structure[15]. The other advantages that conducting polymers provided are their flexibility, environmental stability, and chemical inertness[15].

Table 1: Characteristic Comparison of Metals, Plastics, and Conducting Polymers[16]

	Metals	**Plastics**	**Conducting polymers**
Electrical property	Conductors	Insulators	Conductors
Processibility	Difficult	Easy	Easy
Optical property	Colorful/ shining	Colorless	Colorful/ shining
Other property	Hard/tough	Soft/flexible	Soft/flexible

The conductive ability of these polymers can be attributed to the extended conjugated π-bond structure along their backbone chain[15], which is explained by the Homo-Lumo (band gap) theory. In order to obtain higher conductivity in organic semi-conductors, a longer conjugated π-

bond backbone structure is necessary. In this case, lower energy is enough for charges to move through the bands with less energy difference. This means that the energy difference between the lowest unoccupied molecular orbital, the conduction band, and the highest occupied molecular orbital, the valence band, will be lower as the π-bond structure becomes longer for these polymers. A schematic explanation of band gap can be seen below in Figure 10.

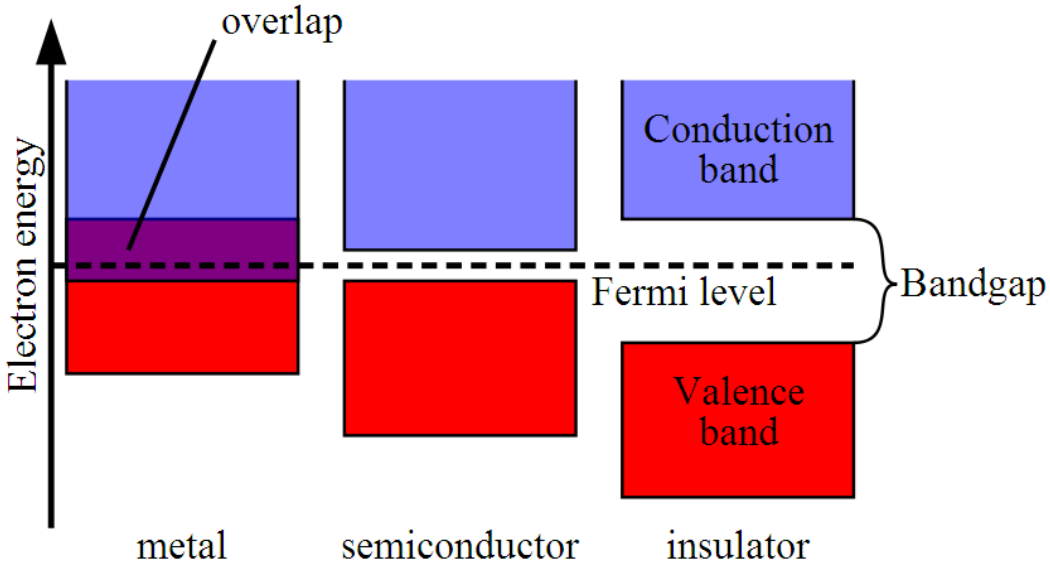

Figure 10: Electronic Band Structure[17]

Some conducting polymers, along with their correlating band gaps, can be seen in below in Figure 11.

Polymer (date conductivity discovered)	Structure	π–π* gap (eV)	Conductivity# (S/cm)
I. Polyacetylene and analogues			
Polyacetylene (1977)	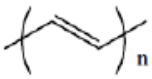	1.5	$10^3 - 1.7\times10^5$
Polypyrrole (1979)	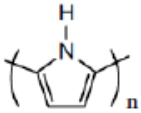	3.1	$10^2 - 7.5\times10^3$
Polythiophene (1981)	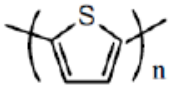	2.0	$10 - 10^3$
II. Polyphenylene and analogues			
Poly(paraphenylene) (1979)	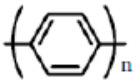	3.0	$10^2 - 10^3$
Poly(p-phenylene vinylene) (1979)	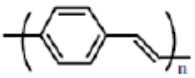	2.5	$3 - 5\times10^3$
Polyaniline (1980)	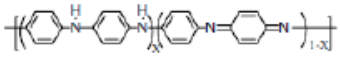	3.2	30 – 200

Figure 11: Several Conducting Polymer structures, along with their band gap and conductivity[18]

Conducting polymers can be synthesized through different types of polymerization reactions such as chemical oxidative polymerization, electrochemical polymerization, photochemical polymerization, plasma polymerization and organic synthesis[19]. The chosen method of synthesis for this study was a chemical oxidative polymerization, where an oxidant is added to the monomer in an aqueous solution in order to oxidize the monomer. Oxidants that can be used include: ammonium peroxydisulfate ($(NH_4)_2S_2O_8$), hydrogen peroxide (H_2O_2), ferric chloride ($FeCl_3$), potassium permanganate ($KMnO_4$), potassium dichromate ($K_2Cr_2O_7$) and potassium perchlorate ($KClO_4$)[16].

1.4.2.1 Polypyrrole

Polypyrrole (PPy) is one of the most widely investigated conductive polymers because of the aqueous solubility of the monomer, the low oxidation potential and high conductivity. Because of those characteristics, PPy has been investigated for many potential applications such as antistatic, electromagnetic shielding, actuator, polymer batteries and corrosion protection[20].

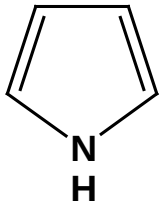

Figure 12: Chemical Structure of the pyrrole monomer

The most common methods applied to synthesize polypyrrole are the chemical oxidative polymerization with doping, electrochemical polymerization, plasma polymerization, and the organic synthesis. A diagram of pyrrole polymerization through a chemical oxidative polymerization can be seen in Figure 13. The process begins through the oxidation of the pyrrole monomer forming a radical cation. This occurs with the presence of an oxidant such as Ammonium Persulfate (APS), $(NH_4)_2S_2O_8$ or Ferric Chloride, $FeCl_3$.The radical cation that is formed has the ability to form the resonance structure seen below. This resonance structure is suitable for oxidative coupling with another present resonance structure. Upon coupling, an intermediate dimer structure is formed. The elimination of hydrogen then takes allowing for the formation of a much more stable dimer structure that is seen below. The process continues to repeat itself until the monomer is exhausted. When the polymerization takes place in DI water, the final dimer structure is the structure seen just after the elimination of hydrogen. When the polymerization takes place in an acidic solution, such as 1M HCl, it allows for the presence of a

chlorine counter ion. The presence of the chlorine ion creates a much more electrically conductive polymer by allowing electrons a pathway to travel through the polymer.

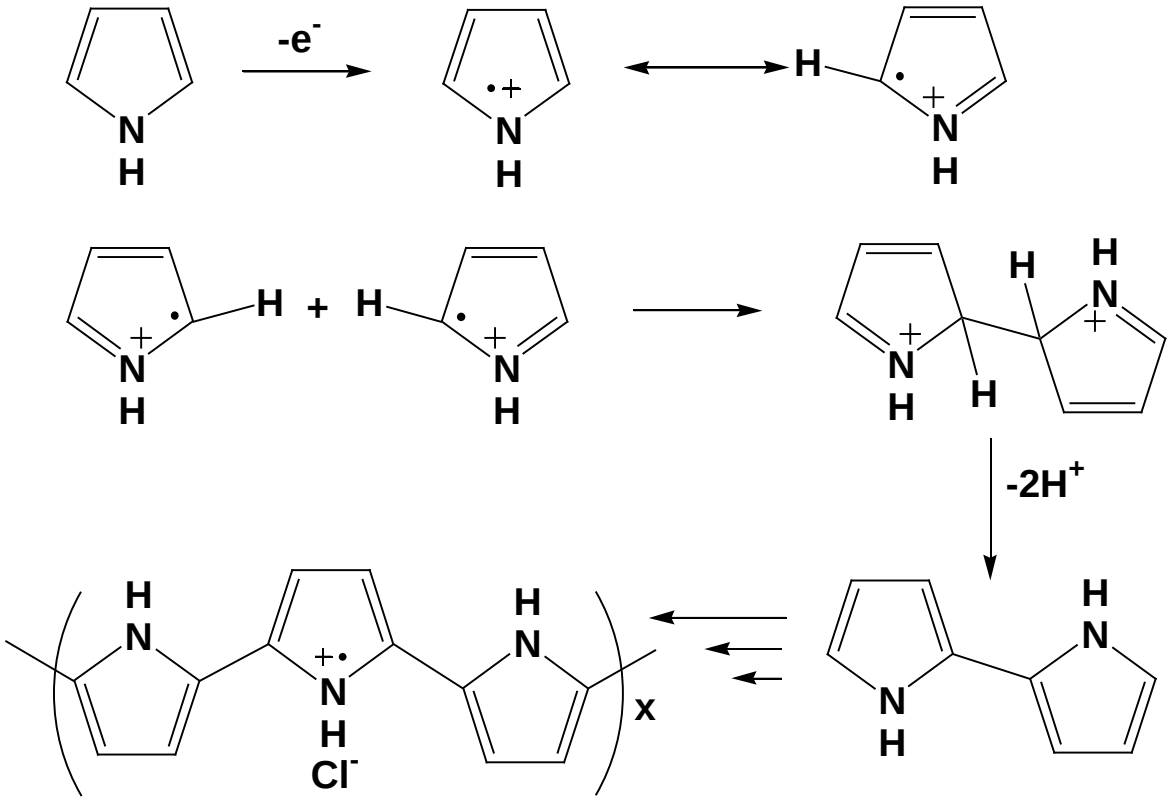

Figure 13: Chemical oxidative polymerization and doping process of pyrrole[17]

CHAPTER 2

SYNTHESIS OF ORGANIC NANO-CONDUCTORS AND CONDUCTOR/EPOXY COMPOSITES

2.1 Introduction

This chapter will discuss the synthesis of organic nano-conductors, their exposure to microwave irradiation, and their incorporation in epoxy composites. Conducting polymer fillers will be synthesized and also used for a conducting coating on milled carbon fiber. These fillers will eventually be mixed with a metallocene catalyst in a 1:1 ratio and exposed to microwave irradiation. Microwave irradiation should provide enough energy for the growth of CNTs on the surface of these materials to create multi-dimensional filler.

In a second effort for nano-conductor synthesis, carbon fiber fabric will be soaked in a metallocene loaded solution then also exposed to microwave irradiation. In Chapter 3, these microwave treated fabrics as well as the above mentioned fillers will be viewed under SEM to determine CNT growth quality and overall coverage.

Lastly, carbon heavy solvents will be added before microwave irradiation just after metallocene introduction to determine their role in possible improvements in CNT quality and coverage. By adding more carbon molecules to the reaction, the goal is to improve CNT growth and coverage.

2.2 Experimental Section

2.2.1 Materials

For polypyrrole fiber and granule synthesis, pyrrole (98+%), ammonium peroxydisulfate (APS $(NH_4)_2S_2O_8$) 98% were purchased from Alfa Aesar and used as received. Deionizaed (DI) water and 1M HCl were used as aqueous media in the polymerizations.

To ensure PPy fiber formation, ammonium metavanadate (NH_4VO_3) 99.5% from ACROS ORGANICS and DOWEX® MARATHON (H) ion-exchange resin from Sigma Aldrich were purchased to prepare V_2O_5 sol-gel nanofibers within Deionized (DI) water, according to the following process (in 160mL DI water + 0.8g NH_4VO_3 + 8g Dowex resin were mixed together without any shaking or magnetic stirring and allowed to sit undisturbed for 2 weeks' time).

In addition, as a substrate for PPy coating, 60 μm milled Carbon fiber was selected. The milled carbon fiber was purchased from Toho Tenax America by Teijin. Also mentioned above, carbon fiber fabric was used as a second substrate for CNT synthesis. The fabric chosen was a 2x2 twill weave purchased from Sigmatex.

For the purification of final polymeric and nanocomposite structures, acetone (BDH®) $(CH_3)_2CO$ was purchased from VWR and used with DI water and 1M HCl.

Several materials were selected and used in the synthesis of CNTs. Ferrocene, $Fe(C_5H_5)_2$ was the metallocene catalyst of choice and was purchased from Alfa Aesar. The carbon heavy solvents that were selected were Tetrahydrofuran, C_4H_8O, Hexane, $CH_3(CH_2)_4CH_3$, and Ethyl Alcohol, CH_3CH_2OH. Both Tetrahydrofuran and Hexane were purchased from VWR, while Ethanol was purchased from EMD.

For epoxy sample preparation, Epon 862 epoxy resin was selected for composite preparation and purchased from Momentive. Below is a figure depicting the chemical structure of Epon 862.

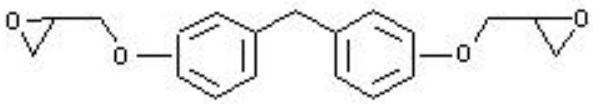

Figure 14: Chemical Structure of Epon 862 Resin

Epikure 3230 was chosen as the hardener to be paired with the Epon 862 resin and was also purchased from Momentive. Figure15 shows the ideal chemical structure of the Epikure 3230. The resin and hardener were mixed in a 100:35 ratio. This was the suggested ratio provided by Momentive.

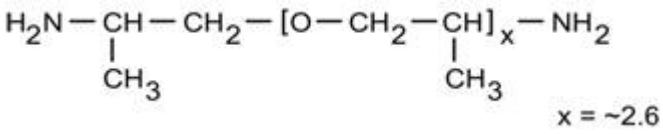

Figure 15: Chemical Struture of Epikure 3230 Hardener

2.2.2 Synthesis Methods

This section describes the synthesis methods used to create nano-conductors using different substrates. The synthesis of Polypyrrole will be discussed, including the synthesis of two different polymer morphologies using both distilled water and 1M HCl. Another filler will be discussed when milled carbon fiber is added to synthesis of the conducting polymers to result in a conductive polymer coating on the surface of milled carbon fiber. The purification of stated samples will be discussed followed by detailed descriptions of the microwave assisted carbonization process. Microwave assisted carbonization is attempted with hopes of producing a 3-D filler through growth of carbon nanotubes. Microwave assisted carbonization is also applied to carbon fiber fabrics in attempt to growth CNTs directly to the surface of the fabrics. Finally,

the preparation of epoxy composite samples using the fore mentioned materials in combination with the synthesized fillers will be explained.

2.2.2.1 Synthesis of Polypyrrole (PPy) Granules and Fibers

Two different PPy structures, granular and fibrillar, were prepared in the presence of milled carbon fiber to create a substrate for carbon nanotube growth. It will be shown in the next section through SEM that both morphologies can be synthesized in each distilled water and HCl, respectively.

2.2.2.1.1 Polypyrrole Granules

Polypyrrole (PPy) granules can be synthesized in two different aqueous media, DI water and HCl. For synthesis, which can be seen below in Fig. 13, 60 mL of either aqueous media was needed. While subjected to magnetic stirring, 1 mL of pyrrole was gently added to the aqueous media. The mixture was stirred for 5-10 min to ensure a uniform dispersion of the pyrrole monomer which created a light yellow solution. After the 5-10 min of stirring, 1.15g of APS, the oxidant, was added to the solution and the color changed from light brown to black due to the formation of PPy structures. The solution was allowed to stir for an additional 3-4 hours to ensure maximization of monomer conversion to polymer.

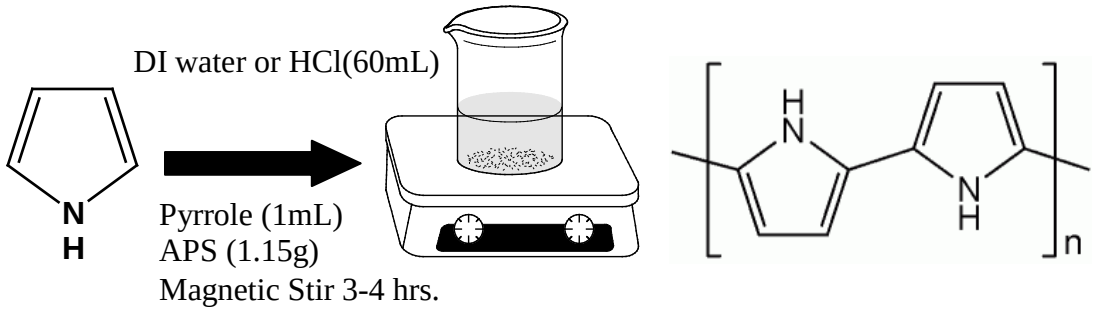

Figure 16: PPy Granule Synthesis

2.2.2.1.2 Polypyrrole Fibers

Preparation of Fibrillar PPy is synthesized in a similar fashion to PPy granules. The synthesis starts with 60 mL of DI water or HCl. For water, 1 mL of V_2O_5 sol-gel nanofibers was added to the 60 mL of water under magnetic stirring. The 1 mL of pyrrole monomer was added to the solution within 1 min so that the V_2O_5 and pyrrole would initiate and maintain the fibrillar structure for the resulting PPy structures. Lastly, 1.15g of APS was added to the solution to initiate polymerization. A color change was noticed when the polymerization began changing the pre-polymerization color from greenish yellow to black. The polymerization was allowed to stir 3-4 hours to ensure completion of the polymerization.

For PPy fiber in HCl, the order of adding components changed due to V_2O_5 sol-gel's inability to survive in an HCl environment. To begin, 1 mL of pyrrole is added to 60 mL of aqueous HCl under magnetic stirring. After the pyrrole is allowed sufficient time to disperse into the aqueous HCl, 1 mL of V_2O_5 was added to the solution. To ensure resulting fiber morphology, 1.15g of APS was added, within 1 min, to initiate the polymerization. A similar color change is noticed in the HCl polymerization compared to the polymerization completed in DI water. Finally, the solution was stirred 3-4 hours to ensure completion of the polymerization. A schematic for PPy fiber polymerization can be seen below.

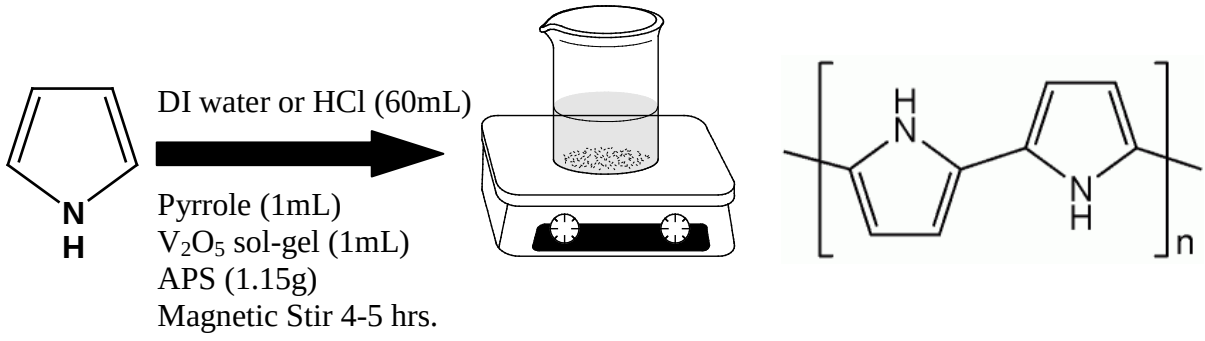

Figure 17: PPy Fiber Synthesis

2.2.2.2 Synthesis of PPy Coated Milled Carbon Fiber (PPy/MCF)

Milled Carbon fiber (MCF) is coated with PPy to increase potential of CNT growth and the conductivity of the MCF itself. The procedure is identical to those above for both granule and fiber morphologies, except MCF were present in the solution while the polymerization took place. 1g of milled carbon fiber was placed into 60 mL of HCl or DI water. Each step after that was identical to the previous mentioned synthesis methods. For instance, for PPy granules in DI water, the steps are as follows: 1g MCF was added to 60 mL DI water under magnetic stirring, followed by the addition of 1mL pyrrole, stirring for 5-10 min, finally 1.15g of APS was added and 3-4 hours of stirring.

2.2.2.3 Purification of As-prepared Samples

At the end of the specific polymerization times (4-5 hours for PPy granule and fiber and 24 hours for the nanocomposite samples) all different types of reaction solutions containing the black precipitates of polymeric structures and/or nanocomposites went through the same purification process. Each and every prepared sample was washed and suction filtered, in a Buchner funnel, which was attached to a water respirator. A Whatman 70mm diameter filter paper was placed inside the funnel and wet with the appropriate aqueous media. The samples were washed with copious amounts of HCl or DI (3x100mL). This step was performed to remove any residual monomer. Acetone was then used to wash the samples (3x100mL) to remove any low molecular weight organic intermediates and oligmers from the system. This filtering process also expedited the drying process of these prepared samples. The acetone assisted in removing water molecules from the sample to allow for faster drying of the sample. The black precipitates were allowed to air dry (5-10min.) within the funnel until there was no

more liquid present. Finally, the filter paper was removed from the funnel and allowed to dry overnight at standard laboratory conditions.

2.2.3 Microwave Initiated Carbonization (MIC)

Some of the major carbon nanotube synthesis methods were discussed in Chapter 1. The major issues with these synthesis methods include: inert gas protection, complicated instrumentation, long periods of high energy density, and insoluble template use, and difficulty of bulk synthesis. Microwave initiated carbonization solves many of these issues. This synthesis method does not use inert gas, has short microwave irradiation times, and has the potential to be scaled up for larger production runs. The other major benefit that MIC provides is the ability to increase the surface area through CNT growth.

Like previously stated, MIC requires a conductive substrate and a metallocene catalyst. For this study, two main conductive substrates will be used, a conducting polymer, PPy, and carbon fiber fabric. The metallocene catalyst that was chosen was Ferrocene, which, in the past, has proven to be efficient in generating sufficient CNT growth.

When subjected microwave irradiation, the blend of ferrocene and PPy or carbon fiber fabric, depending on which is chosen, absorbs the microwave energy and rapidly heats up causing the ferrocene to react. The samples were exposed to microwave irradiation, from a conventional microwave oven, at short times ranging from 1 min to 1.5 min at a power level of 1250 watts.

2.2.3.1 PPy and PPy/MCF Samples

For microwave initiated carbonization, the previously mentioned samples where dry-mixed with a metallocene catalyst, Ferrocene, and subjected to microwave irradiation. PPy granules, fibers, and PPy/MCF were weighed so that a 1:1 weight ratio was made between the

synthesized material and metallocene catalyst. After achieving a 1:1 ratio for each subset, both the material and catalyst were combined in a plastic mixing cup and speed mixed at 3000 rpm for 1.5 min to ensure even scattering of the metallocene catalyst. Once speed mixing is complete, the mixed material was transferred into a 20 mL glass vial for the microwave carbonization step. The 20 mL glass vial filled with a 1:1 mixed ratio of conducting polymer substrate and metallocene catalyst was placed in the microwave toward the outer edge of the circular glass microwave plate. The microwave was set at full power and a time of 1 min before it was started. Within 10-15sec of starting, a reddish-orange glow was seen and continued to flicker throughout the microwave process. It was important to ensure that the glass vial was loosely sealed to ensure that the gas produced by the burning of the sample was contained within the vial. The final product after microwave irradiation of the mixture is a light to dark gray powder that was characterized by SEM.

In addition to the standard microwave irradiation process mentioned above, improvements can be made. For instance, small organic molecules can be added to the process to provide better growth and coverage of CNTs. Two of the organic molecules that were used were Hexane and Ethanol, in liquid form. Approximately 1 mL of these small organic molecules were added to the glass vial and sufficiently stirred just before microwave irradiation began. When subjected to microwave irradiation, the reaction was more active and lively than the standard method. There were brighter flashes, ranging from yellow to white, and more of them. These samples were also observed under SEM.

2.2.3.2 Carbon Fiber Fabric

For MIC of carbon fabric samples, the procedure was different than previously stated. The carbon fiber fabrics were soaked in acetone for 12 hours to assist in removal of any potential

sizing that may have been present on the surface of the fabric's fibers. After doing so, a 0.5M solution of ferrocene in toluene was prepared. This was done by adding 93.02g of ferrocene to 1L of toluene under magnetic stirring. The solution was stirred for 30 min to allow sufficient time for the ferrocene to partly dissolve in the toluene. The idea behind dissolving ferrocene in solution was to create smaller ferrocene molecules for enhanced dispersion of the metallocene catalyst on the surface of the fabric before microwave irradiation was introduced. Once the ferrocene-toluene solution was sufficiently homogeneous, the solution was poured into an aluminum pan, and the actetone-treated fabrics were placed in the solution. The fabric was allowed to soak in the solution for 30 min before their removal. Once removed from solution, the fabrics were completely dried at standard laboratory conditions before being subjected to microwave irradiation. This typically took approximately 5-10 minutes. The fabrics were exposed to microwave irradiation for 1.5 min. Small samples were cut and placed on aluminum stages for observation under SEM.

The effect of hexane, ethanol, and THF addition was also observed in these samples in order to track potential improvements in CNT quality and coverage. After removal from the Toluene-Ferrocene solution and sufficient drying occurred, 0.5mL of the corresponding solvent was distributed onto each side of the fabric and allowed to semi-dry before exposure to microwave irradiation. The leftover solvent was to aid in increasing the reactivity of the fabric upon microwave irradiation and improve the coverage and growth of carbon nanostructures on the surface of the fabric. After the samples were prepared, small samples were also cut from these and placed on aluminum stages for SEM observation.

2.2.4 Preparation of Standard Epoxy Composite

Preparation of the neat epoxy system was relatively straightforward. Like previously stated in the materials section, Epon 862 was chosen as the resin while Epikure 3230 was chosen as the hardener to be paired with Epon resin. The ratio of resin to harderner was provided by Momentive and was 100 parts resin to 35 parts hardener. Initially, the process was simply adding the appropriate amounts of each and hand stirring for 15 min. After the stirring, the mixture was allowed to cure at room temperature for 7 days. Room temperature curing was chosen to simplify the process. The process for the neat Epon samples was altered later due to settling of filler by hand stirring and will be explained in the next section.

2.2.5 Preparation of PPy coated MCF/Epoxy Composites

For the PPy-MCF epoxy composites, the same hardener to resin ratio was used. The filler weight ratio that was used correlating to the weight of the resin itself. The weight ratio of filler chosen was 3% by weight. When adding nanostructures by themselves, typically, weight ratios are less than 1% by weight. For micron sized particles or fibers, weight ratios can vary. Since reducing the resistance to improve the electrical conductivity was a major concern, it was necessary to use more than 1% by weight. Three percent seemed to be a middle ground between 1-5% that would create for a bridge for electrical current to travel.

Like previously mentioned, 100 parts resin were used to 35 parts of hardener. The resin was weighed out and placed in a 250 mL beaker. The beaker was placed on a hot plate set to 120˚C and allowed to heat for 10 min. The internal temperature of the resin never exceeded 50˚C. By increasing the temperature, the resin's viscosity was decreased allowing for an easier introduction of filler. The appropriate amount of filler was measured and added to the beaker. A magnetic stir bar was added and the contents were mixed at half speed on a magnetic stirrer for

10 min. After stirring, the beaker was placed in a vacuum oven. Vacuum was applied, at room temperature, at a rate of 30 psi for 10 min to assist in removing air bubbles created by stirring in the filler. The beaker and its contents were removed from the vacuum oven and the corresponding amount of hardener was added. The beaker was once again placed onto the magnetic stirrer and stirred for 2 hours until the mixture's viscosity became viscous enough to prevent settling of the filler.

The corresponding neat Epon samples were prepared in a similar fashion. The correct amounts of resin and hardener were placed into a 250 mL beaker and magnetic stirring was introduced. The contents of the beaker were allowed to stir for 3 hrs to ensure a homogenous mixture of resin and hardener and to maximize the amount of crosslinks present in the composite. Finally, the composites were poured into plexi-glass molds and cured at room temperature for 7 days.

CHAPTER 3

RESULTS AND DISCUSSION

3.1 Introduction

In this chapter, different characterization methods were used to gain a better understanding of the base substrates as well as the synthesized materials. The goal was to prove the growth of CNTs and understand their potential as fillers for epoxy composites. Once epoxy composites were created using these fillers, the composites were also analyzed. The examination of the composites was to gain an understanding of the synthesized materials as a filler in a real world application.

3.2 Instruments and Characterization Methods

Scanning Electron Microscopy (SEM) was initially used to characterize the surfaces of the base substrates and the treated substrates. After microwave irradiation was introduced, SEM assisted in analyzing the effect of microwave on the samples and the presence of carbon nanostructure growth.

Although not a major point of characterization for this thesis, an Instron Universal Tensile tester was used to track pretreatment and microwave assisted growth's effect on the strength of the individual fibers within the treated fabrics. This was done to acquire the best method of pretreatment and microwave times to retain the maximum amount of fiber strength.

Next, Thermogravimetric Analysis (TGA) was completed to understand the thermal stability of the base materials and their treated counterparts. This was executed by tracking each samples major degradation temperature and the total weight loss of the sample.

For the Epon-MCF composite samples, Differential Scanning Calorimetry (DSC) was used to understand the fillers effects on the glass transition and curing of the epoxy composites. TGA was also performed to track the effect of the filler during decomposition of the composite samples. Four probe conductivity was briefly examined to determine if the fillers that were incorporated were able to enhance the electrical conductivity of the composite. Since epoxy tends to be a heavy insulating material, the goal was to reduce to the resistivity of the material and improve the capability of electrons to travel through the sample.

Dynamic Mechanical Analysis was also performed on the Epon-MCF composite samples to determine the storage modulus after the glass transition of the material. This value was used to calculate the crosslink density within the sample to determine the fillers effect on overall crosslinking in the sample.

Finally, two different electrical conductivity testing were preformed. For fabric samples, a two probe volt meter was used to determine the resistance of each sample at multiple regions. Once resistance was determined, the conductivity was calculated using the inverse of the resistivity along with the dimensions of the sample. For the MCF samples, the conductivity was determined by taking a 4 probe measurement using a 4 probe set up by the Micromanipulator Company along with a Keithley 4200-SCS semiconductor characterization system.

3.3 Different Characterization Results and Discussion

In the following sections, different characterization methods were explored. To begin, Scanning Electron Microscopy was used to investigate the visual aspect of the synthesized

materials. The structure of PPy granules and fibers are displayed based on previous work completed by Dr. Xinyu Zhang's research group. As-recieived milled carbon fiber surfaces were viewed as well as the surface after different pretreatment techniques. SEM was also used to characterize the composite of PPy granules/fibers before and after microwave treatment. Carbon fiber fabric was also characterized using SEM before and after carbon nanostructure growth.

3.3.1 SEM Characterization Results of PPy Structures

The PPy structures that were used are characterized below by SEM. An image of both PPy granules and fibers are shown below in Figure 18 and 19. Both of the images shown are PPy that has been polymerized in an aqueous solution of 1M Hydrocholoric Acid. The images are shown to allow for a visual idea of what the polymer structures look like without the presence of MCF.

3.3.1.1 PPy Granules

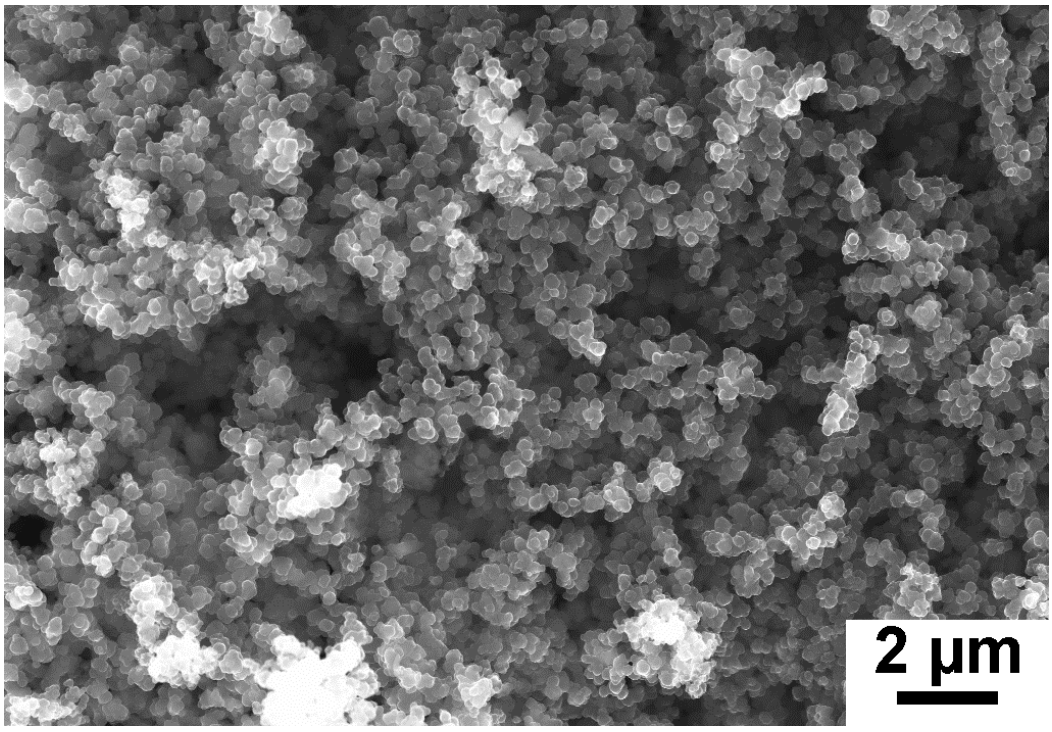

Figure 18: SEM Micrograph of PPy Granules

PPy granules are polymerized by combining monomer and an oxidant in the presence of aqeuous solution. A typical polymerization, like decribed in the synthesis section above, produces an average weight of 0.3g. The granules tend to agglomerate which can also be seen in Figure 18. There is little difference between granules synthesized in HCl compared to DI water.

3.3.1.2 PPy Nanofiber

When the polymerization is carried out in HCl as the aqueous media, it can be seen that the fiber morphology is present as it was when H_2O was the media. The most noticeable difference can be seen in the presence of granules. Due to V_2O_5's vulnerability in HCl, less monomer can be converted to the nanofiber morphology. That is the main difference between the two other than the conductivity tends to be higher in the fibers produced in HCl.

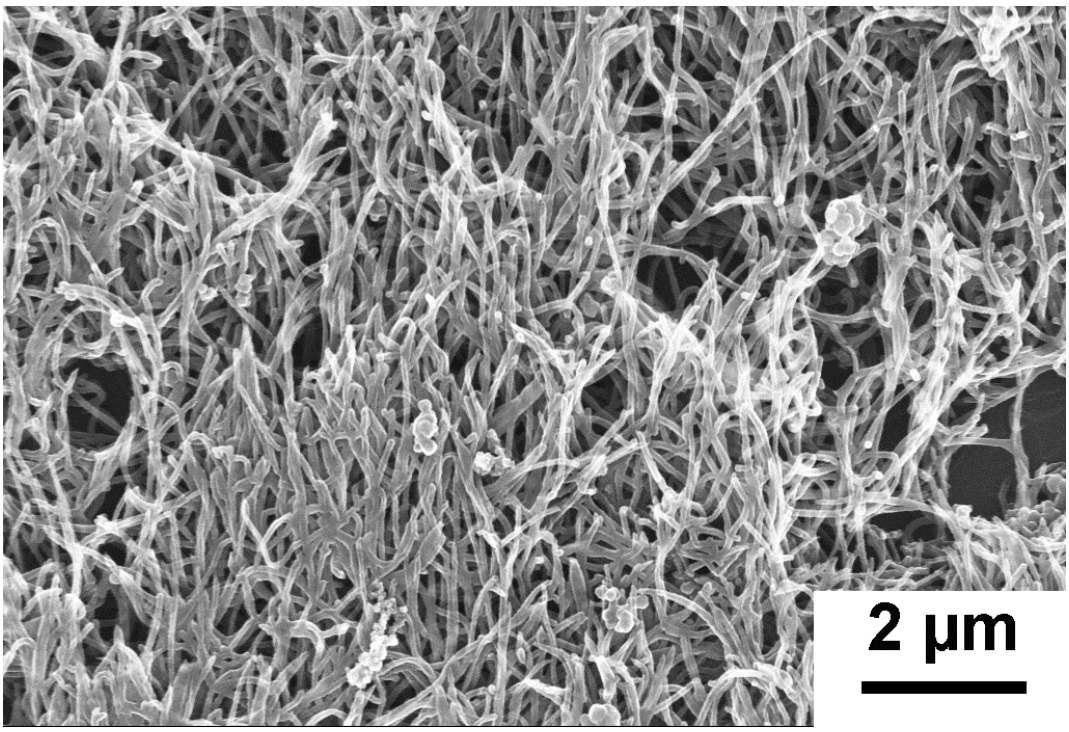

Figure 19: SEM Micrograph of PPy Fiber

3.3.2 SEM Characterization Results of Milled Carbon Fiber

In the sections below, as-received milled carbon fiber and microwave pretreated MCF were characterized by SEM. The surface of the as-received MCF was evaluated while the effects of microwave were evaluated on the microwave pretreated samples. Microwave pretreatment was the only pretreatment method assessed due to the ease and low cost of this pretreatment method.

3.3.2.1 As-Received Milled Carbon Fiber

As seen below, as-received milled carbon fiber had a fairly smooth surface and also what looks to be some debris from the milling process. The debris could be minimized by washing the samples with acetone. Some minimal texture, grooves, could be seen on surface of some MCF. Among examination of multiple samples, it was confirmed that all samples had similar traits.

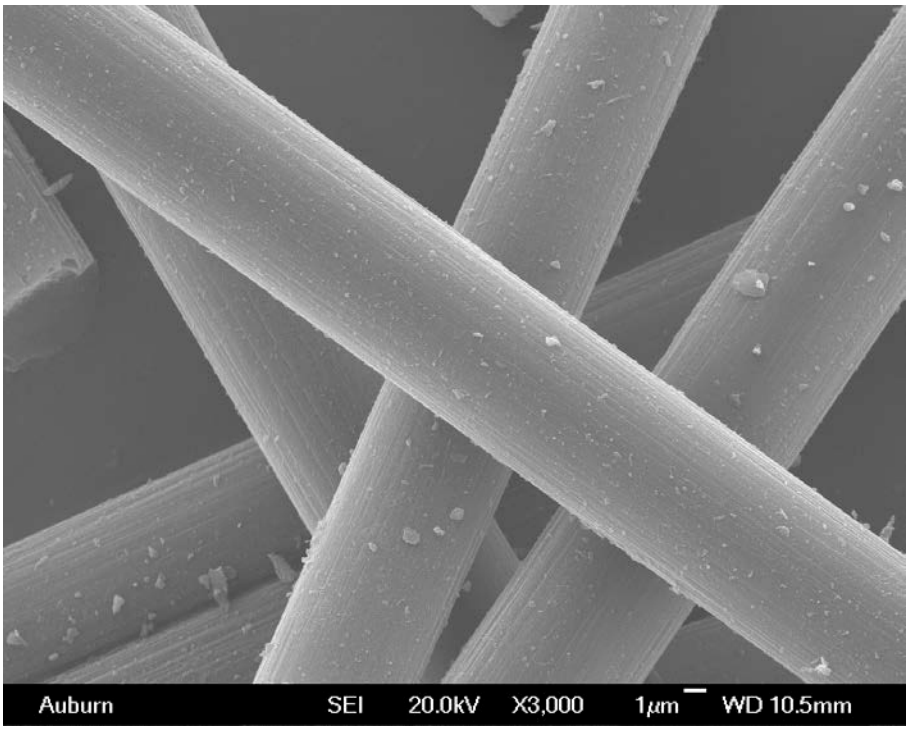

Figure 20: SEM Micrograph of As-Received MCF

3.3.2.2 Microwave Pretreated Milled Carbon Fiber

Pretreatment methods were also attempted on as-received MCF to increase the surface area on the fibers and improve the reactivity of the MCF when microwave irradiation is applied with metallocene catalyst present. Upon microwave pretreatment of only 20 sec, it can be seen that the microwave irradiation was harsh enough to cause major flaws on the MCF surface. This can be seen in Figure 21, below. After noticing the surface flaws caused by the microwave irradiation pretreatment, pretreatment methods were later abandoned as not to compromise the structural integrity of the MCFs.

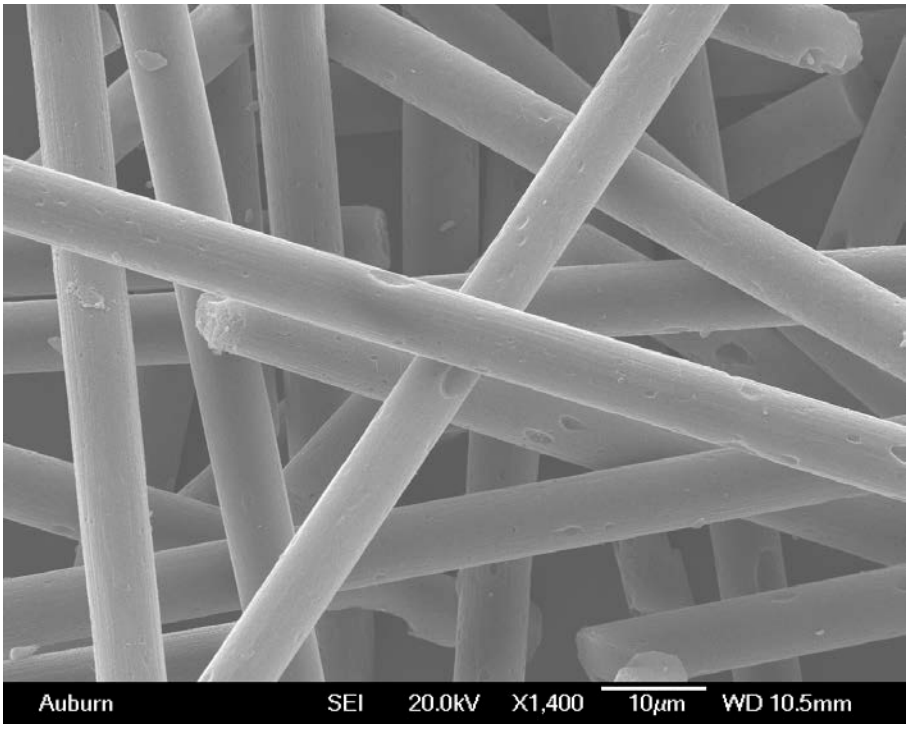

Figure 21: SEM Micrograph of Microwave Pretreated MCF

3.3.3 SEM Characterization Results of PPy- Milled Carbon Fiber Composites

3.3.3.1 SEM Characterization Results of Granular PPy- MCF Composite

In figure 22 and 23, images of the the PPy granule – MCF composites can be seen. In Figure 22, the composite is viewed at a lower magnification allowing for viewing of the overall

homogeneity. Although PPy granules can be seen on or near the surface in Figure 23, Figure 22 shows that granules were not always near or touching the surface of every MCF. This could lead to issues with CNT growth once metallocene catalyst and microwave irradiation are introduced. The effect of the morphology will be explored further in later sections.

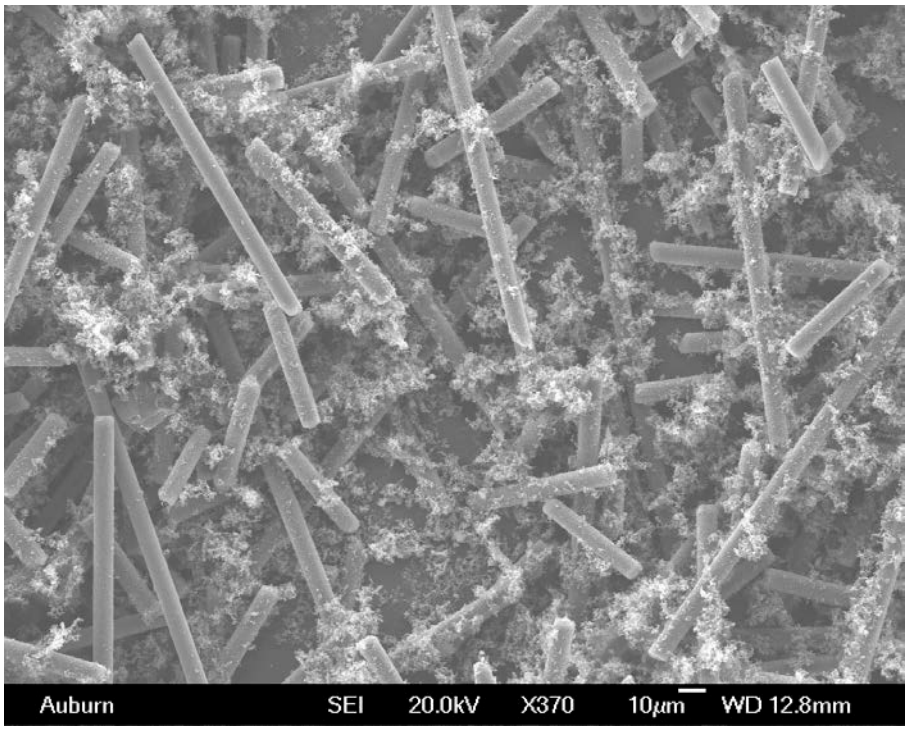

Figure 22: SEM Micrograph of PPy granule-MCF Composite at 370X magnification

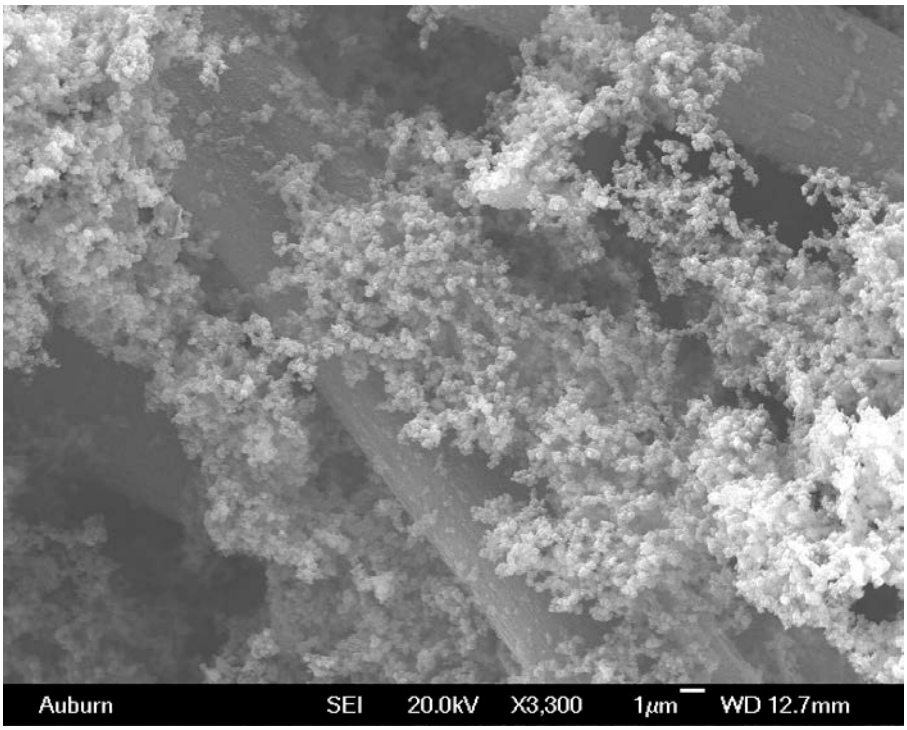

Figure 23: SEM Micrograph of PPy Fiber-MCF Composite at 3300X magnification

3.3.3.2 SEM Characterization Results of Fibrillar PPy Coated MCF

Compared to the PPy granule – MCF composites, the fibrillar version has much more of coating due to the semi encapsulation of the MCFs. Both are homogenous in their own right, but since the PPy fiber has the ability to interlock, the MCF is partial or fully covered by PPy fiber in most cases. Below, in Figure 24, a perspective overview of PPy fiber coverage can be seen.

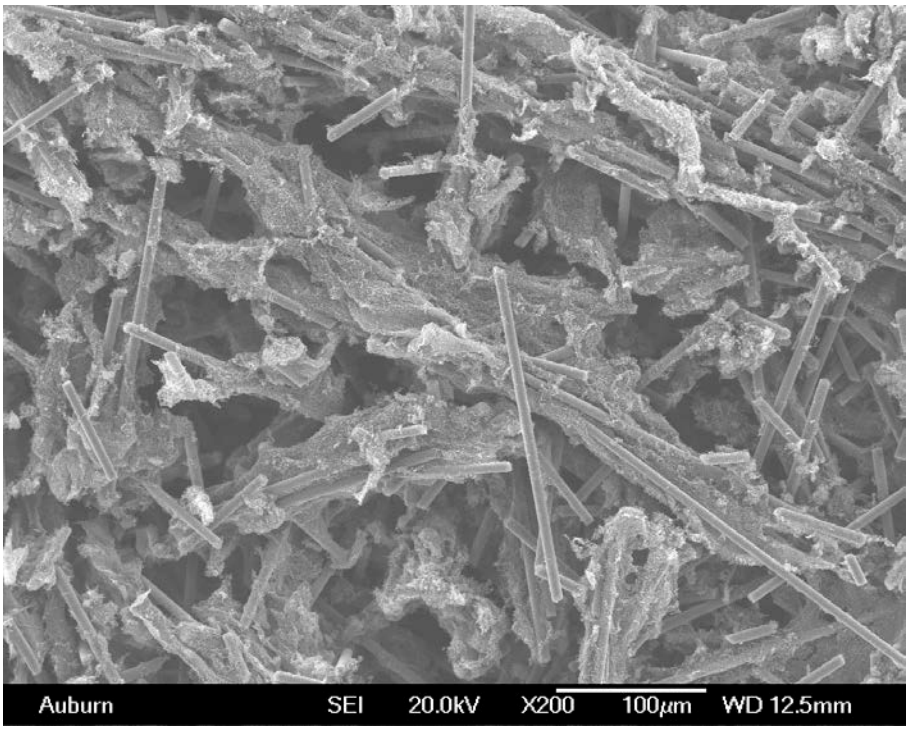

Figure 24: SEM Micrograph of PPy-MCF Composite at 200X magnification

Upon further viewing, Figure 25, depicts a better look at the encapsulation that is discussed above. The interlocking of the PPy fibers can clearly be seen as well as the semi-encapsulation of the MCF. When the metallocene catalyst and microwave irradiation are introduced, it is predicted that the CNT coverage and growth will be improved. The amount of PPy fiber touching the surface of the CNT is much larger than that of the PPy granule-MCF composite which will lead to better growth of CNTs on the surface of the MCFs.

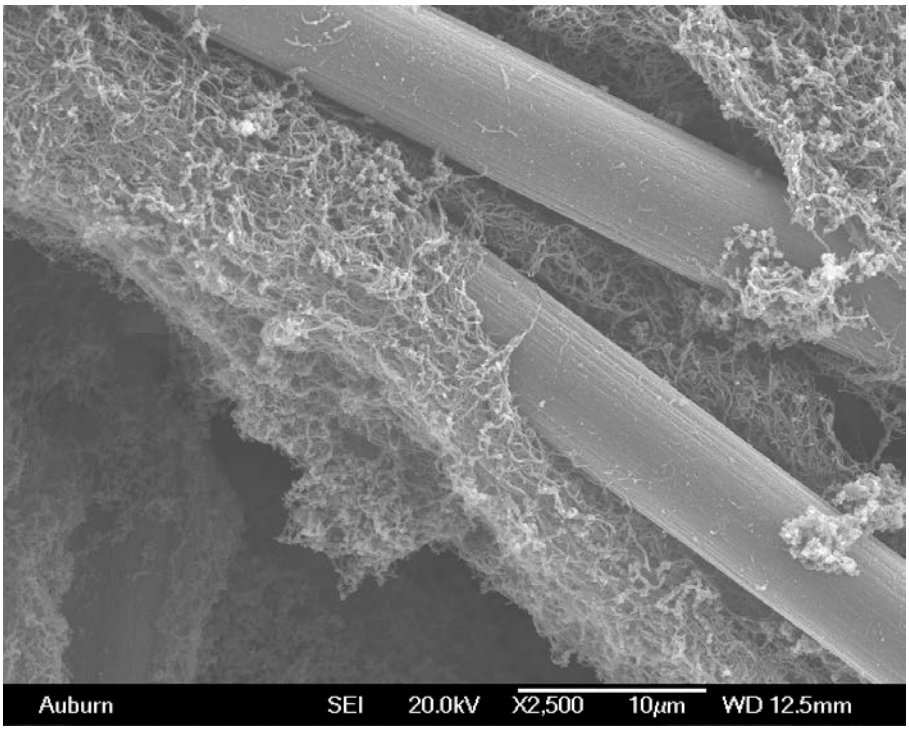

Figure 25: SEM Micrograph of PPy-MCF Composite at 2500X magnification

3.3.4 SEM Characterization Results of Microwave Treated PPy - Milled Carbon Fiber Composites

The following SEM micrographs are from PPy-MCF composites that were mixed with a metallocene catalyst and exposed to microwave irradiation. Both morphologies of PPy, granule and fiber, were used and viewed under SEM observation. The effect of microwave pretreatment was also observed under SEM. The micrographs were used to determine the best growth of CNTs, and the best filler was chosen based on structural intergrity, CNT growth quality, and CNT growth coverage.

3.3.4.1 SEM Characterization Results of Microwave Treated Granular PPy-MCF Composites

In figure 26, it can be seen that the granular structure assists in the growth of CNTs. Although the coverage in the image below seems adequate, this is not a great representation of

the composite as a whole. There were large areas of the sample that upon observation milled carbon fiber had little or no CNT growth. This can most likely be explained by the random dispersion of PPy granules mentioned earlier. Since the granules are not always on or near the surface, this led to large amounts of growth in some regions and not in others. Since the surface of the milled carbon fibers tends to be smooth, the PPy granules are not able to adequately anchor to the surface of the carbon fibers.

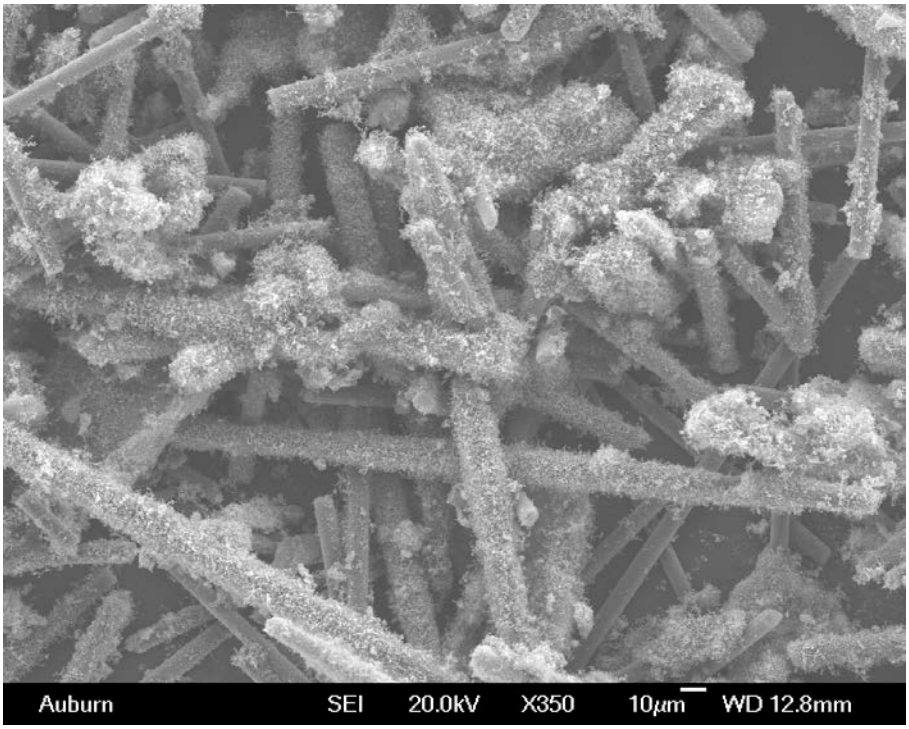

Figure 26: SEM Micrograph of Microwave Treated PPyG-MCF Composite at 350X Mag.

Even though the coverage amongst the entire sample was not ideal, there were areas that showed quality CNT growth. Figure 27 displays two milled carbon fibers that have a homogeneous coverage of CNT growth. The fibers appear to have CNT growth that originated at the surface of the fiber and are completely enclosed by the growth. The coverage on these fibers is superb, yet the CNTs, themselves, do appear to be fairly random and do not display the desired growth pattern. It can be seen that some of the tubes that grew on the surface grew upward then turned in

the direction of the length of the carbon fiber. Ideally, the desired growth would strictly extend outward from the surface directly perpendicular to the area of attachment.

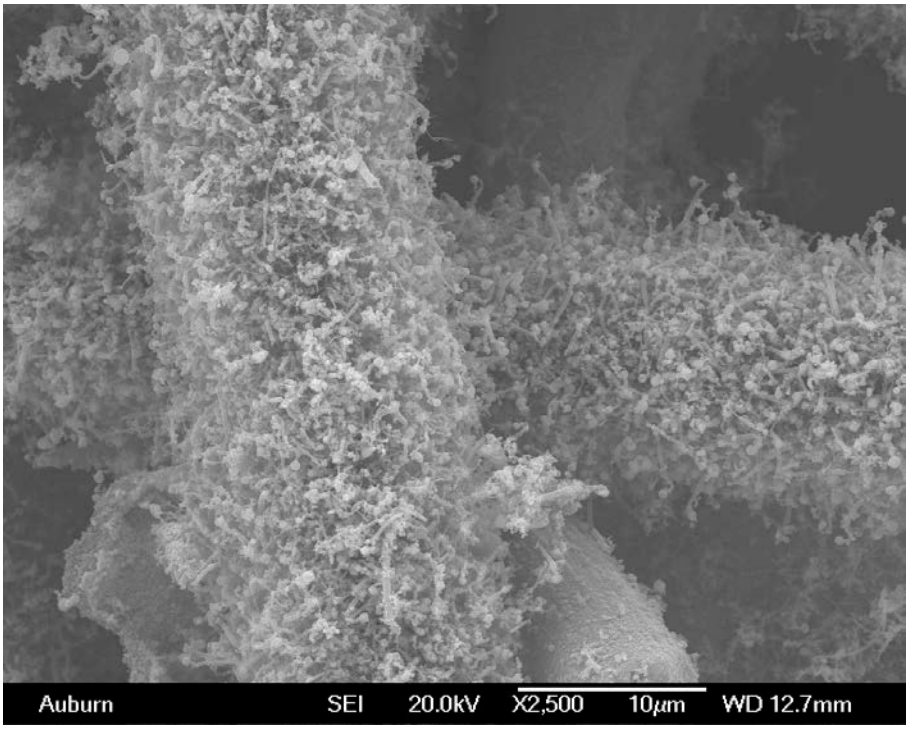

Figure 27: SEM Micrograph of Microwave Treated PPyG-MCF Composite at 2500X Mag.

3.3.4.2 SEM Characterization of Microwave Treated PPy Fiber-MCF Composite

The PPy Fiber-MCF composite also produced quality growth of CNTs. It was actually quite improved as far as overall coverage. This could have been due to large agglomerations that absorbed large amounts of microwave energy and dispersing it to the surrounding areas. Large, homogenous areas are growth were present when observed under SEM. This can be seen in figure 28. Although there are bare fibers present, it is safe to estimate a coverage of approximately 40-60%. This is higher than the granule samples. The coverage percentages on those were lower around 30-40%.

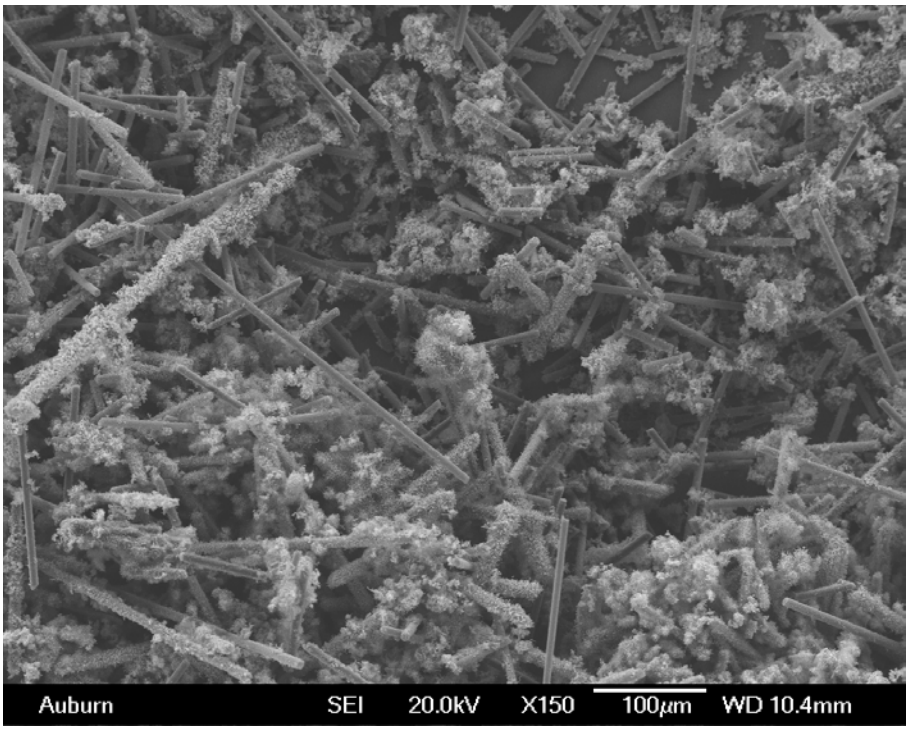

Figure 28: SEM Micrograph of Microwave Treated PPyF-MCF Composite at 150X Mag.

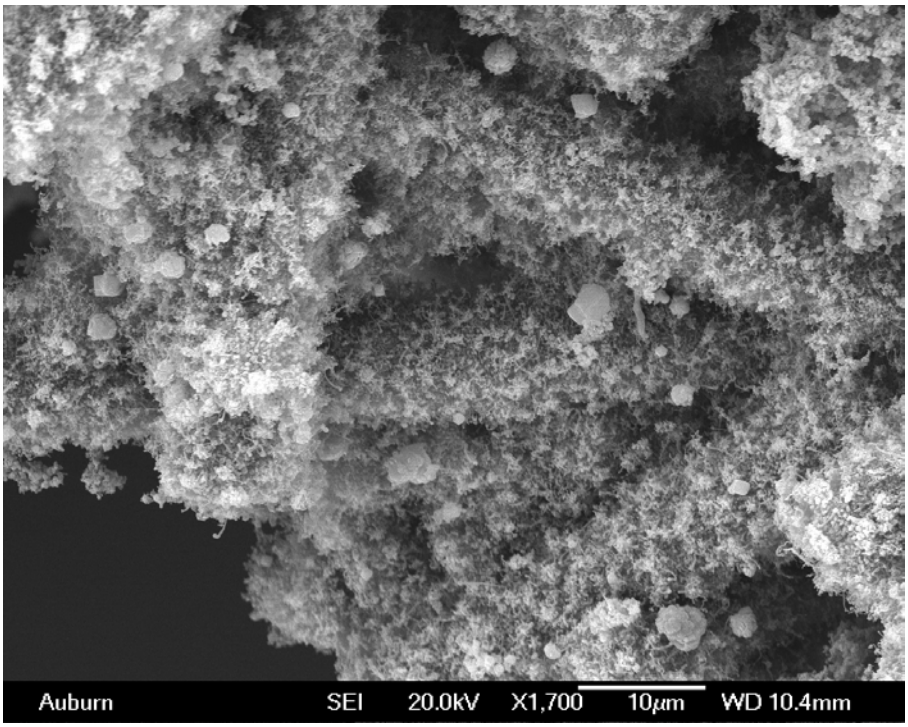

Figure 29: SEM Micrograph of Microwave Treated PPyF-MCF Composite at 1700X Mag.

In figure 29, a higher magnification image can be seen. The MCFs shown are completely covered from end to end with CNT growth with short CNTs. It should be noted that the larger , spherical particles that are ferrocene particles. These were either unable to decompose or were not washed away after filtering the samples and washing them in acetone.

3.3.4.3 SEM Characterization of Microwave Treated Fibrillar PPy- MCF Composite using Microwave Pretreated MCF

In figure 30, large clumps of MCF can be seen. It is also noticeable that large amounts of CNT growth are present on the surface of these fibers. The coverage in this micrograph was far none. It could be estimated that the coverage in this image is approximate 70% or more.

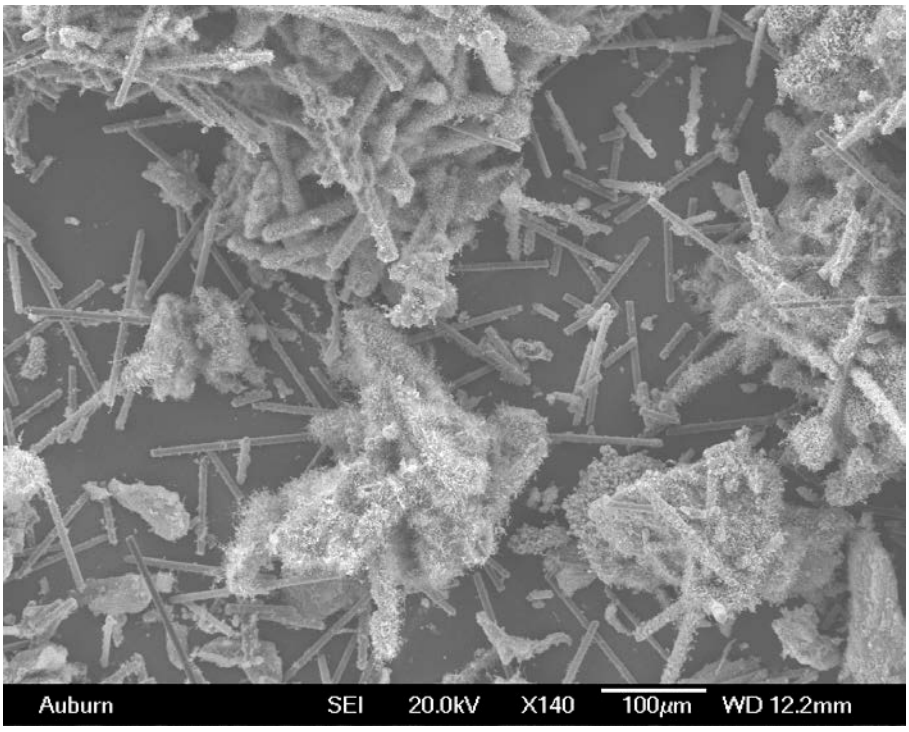

Figure 30: SEM Micrograph of Microwave Treated MPT PPyF-MCF Composite at 140X Mag.

Upon further inspection at a higher magnification, the growth quality, coverage, and density is far better than that of the previously mentioned samples. The CNTs appear to be longer and a thicker coverage is present. When viewing figure 32, it can be seen that the CNTs are several microns in length and have a much more perpendicular growth pattern than previous samples. The iron particles at the end of the tubes can also be clear seen, indicating a tip growth mechanism. Even though the growth is highly improved, it is hard to justify using it as filler due to the large defects that the microwave pretreatment caused on the surface of the fibers. These large defects compromise the structural integrity and mechanical strength of the MCF. That is the reason that these MCF-CNT samples were not used as a filler to characterize the effect of the CNT growth on the filler within the epoxy composite.

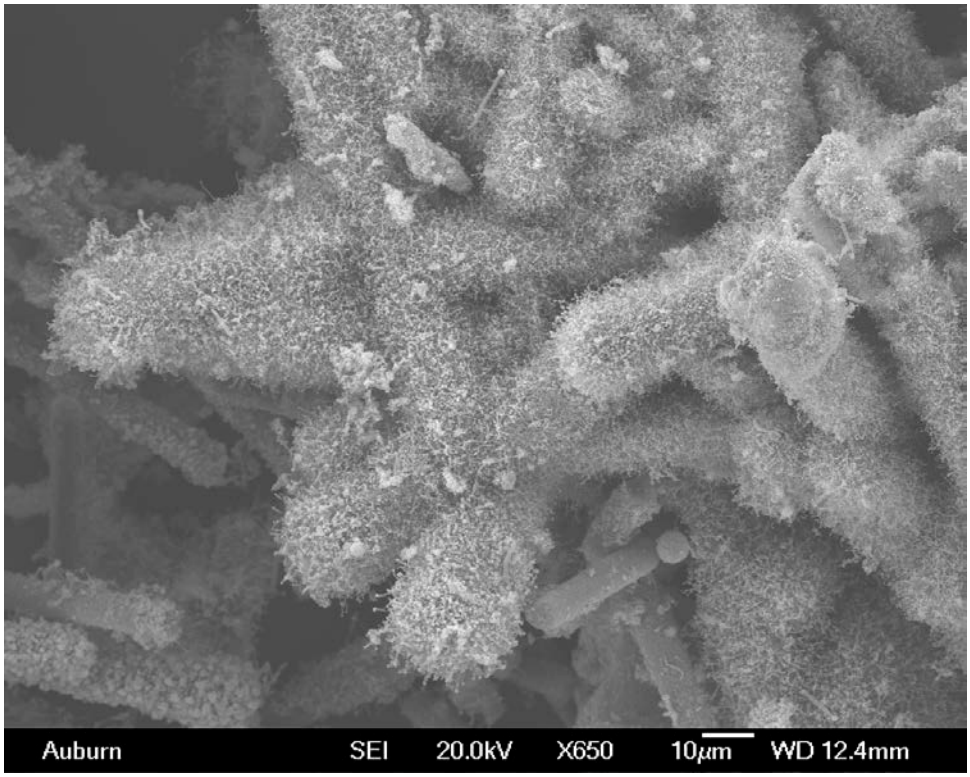

Figure 31: SEM Micrograph of Microwave Treated MPT PPyF-MCF Composite at 650X Mag.

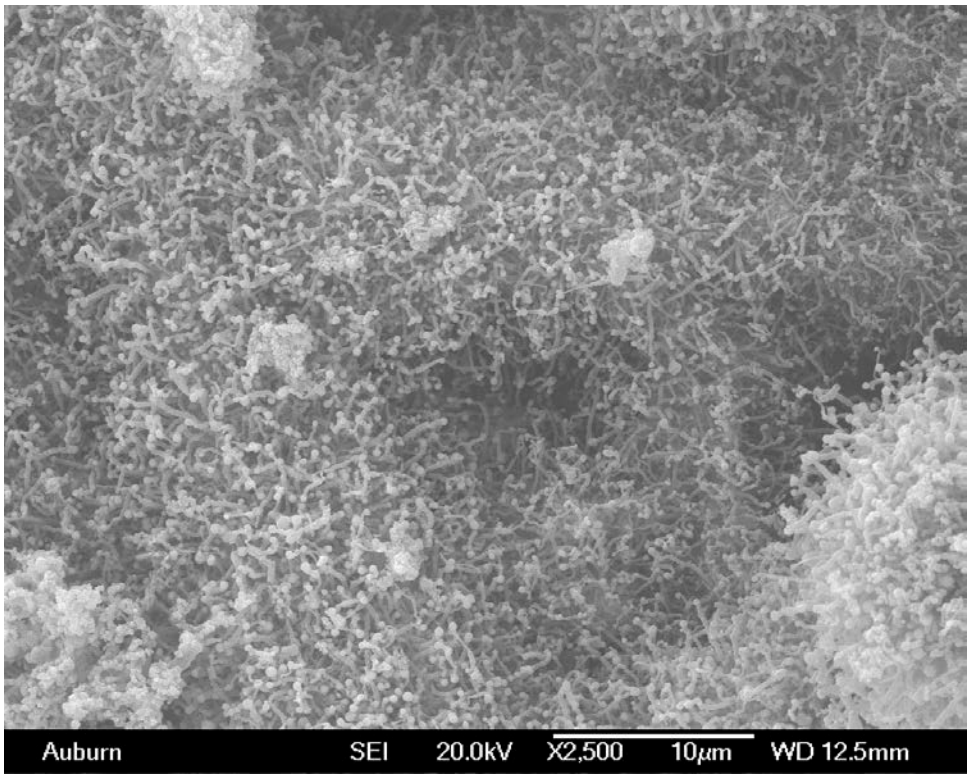

Figure 32: SEM Micrograph of Microwave Treated MPT PPyF-MCF Composite at 2500X Mag.

3.3.5 SEM Characterization Results of Microwave Treated Carbon Fiber Fabrics

3.3.5.1 SEM Results of Microwave Treated CF Fabric

Upon microwave irradiation, the fabric was much more reactive than that of the PPy or milled carbon fiber samples. As one would imagine, the SEM micrographs looked considerably different as well. Where the PPy and milled carbon fiber samples were much harder to control as far as growth quality and coverage, the fabric samples were much more homogenous and produced a considerable amount more of carbon nanostructures, which can be seen in the figure below.

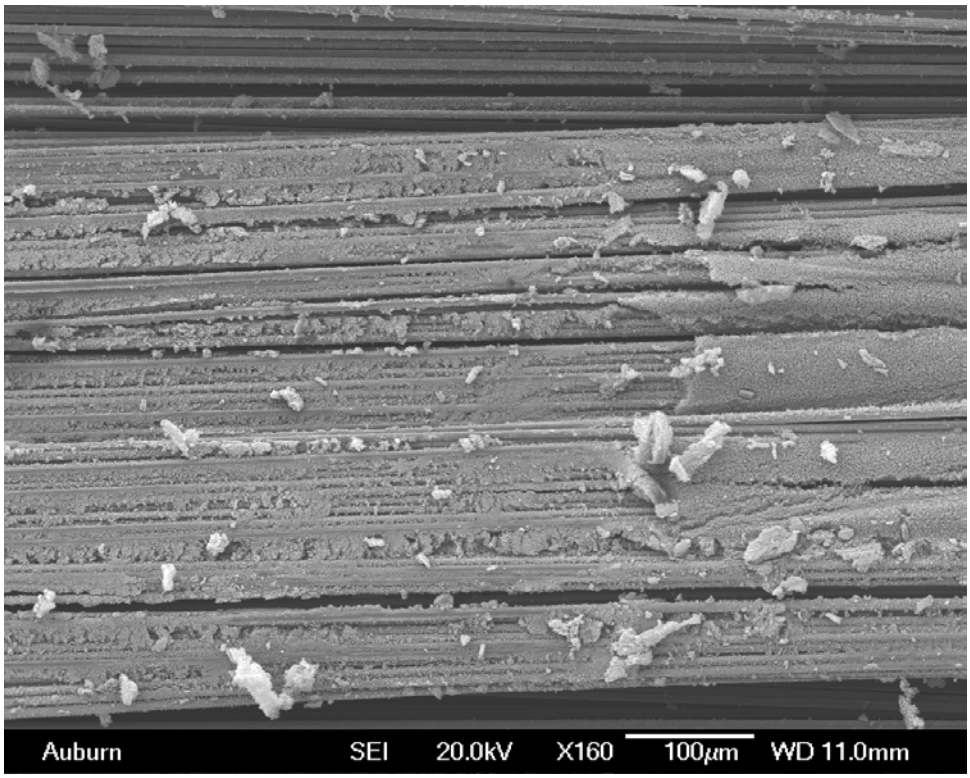

Figure 33: Carbon Fiber Fabric after introduction of catalyst and Microwave Irradiation

It can also be seen that even though there was a significant amount more growth there is still fibers that have little or no nanostructure formation. In low magnifications, the structures resemble CNTs, but when further inspected, the structures were simply large agglomerations of carbon nanoparticles. The lack of nanoparticle and CNT formation could possibly be explained by the sizing that is added to carbon fabrics for improved handling in industrial settings. In order to battle this issue, pretreatment methods were attempted to assist in removal of the sizing and allow for more of the active fiber surface to be exposed during the microwave process.

3.3.5.2 Microwave Treated CF Fabrics with MW Pretreatment (MPT)

Microwave pretreatment was one of the methods used to assist in removal of the fabric sizing. The fabrics were subjected to microwave irradiation for up to 30 seconds before the introduction of the metallocene catalyst solution. In Figure 34, a microwave pretreated fabric can

be seen that was soaked in the ferrocene-toluene solution and microwaved to synthesize carbon nanostructures.

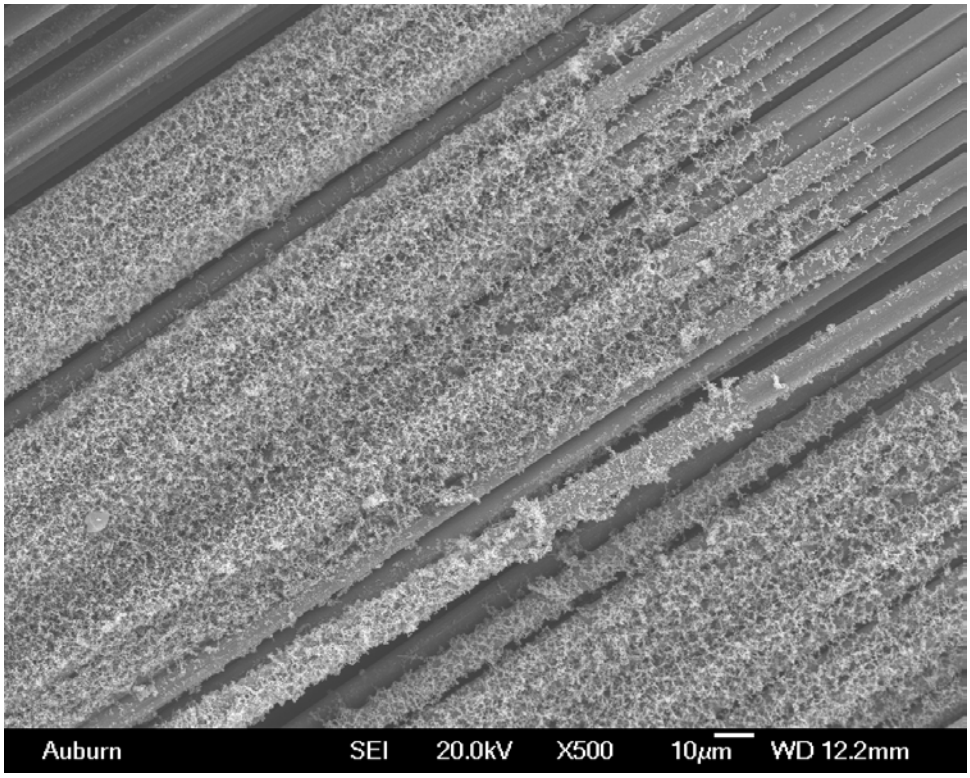

Figure 34: MPT Carbon Fiber Fabric after introduction of catalyst and Microwave Irradiation 1

After microwave pretreatment, the fabric seemed to have provided more active sites for formation to occur. It can be seen that there is a more homogenous formation of nanoparticles, and the clumpy masses that were present before pretreatment have diminished. Upon further magnification, like in Figure 35, a uniform formation of nanoparticles can be seen.

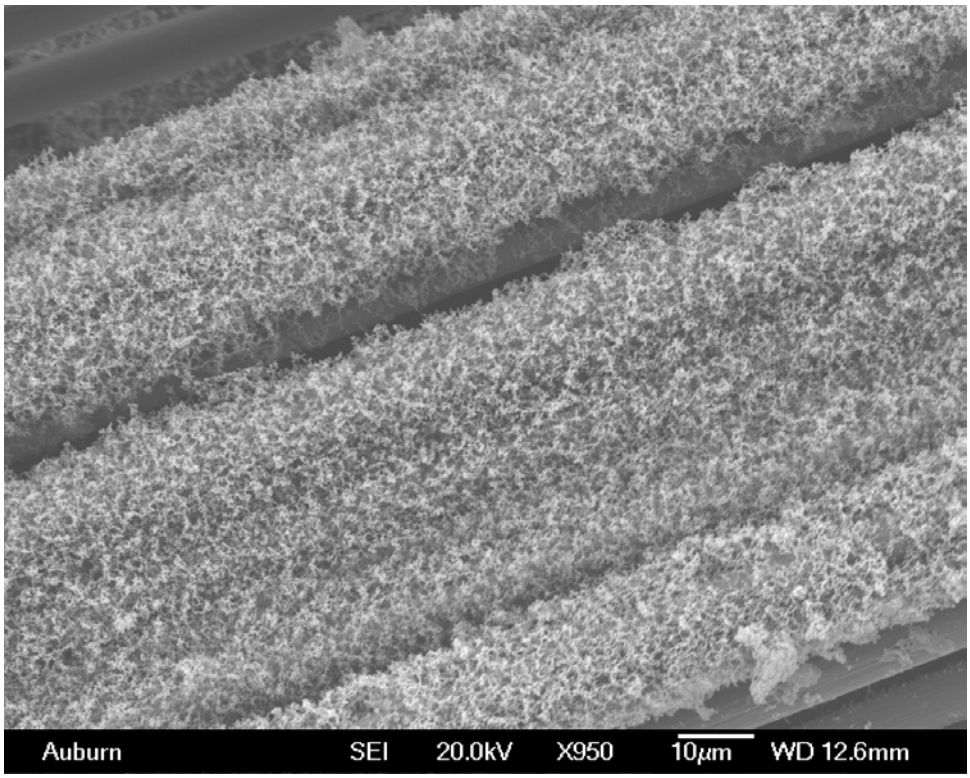

Figure 35: MPT Carbon Fiber Fabric after introduction of catalyst and Microwave Irradiation 2

3.3.5.3 Microwave Treated CF Fabrics with Acetone Pretreatment (APT)

Acetone pretreatment was the second method that was attempted to remove the fabric sizing. Of the two methods, this was seen as a less harsh sizing removal technique. Fabrics were soaked in acetone for 12 hours in order to slowly decompose the fabric sizing. It also assisted in removing any potential debris that was present on the surface of the fabrics.

Figure 36 displays and SEM micrograph, at 550X magnification, of an acetone pretreated fabric after the introduction of catalyst and microwave synthesis. The outcome was closely similar to that of the microwave pretreated samples. The pretreatment provided a uniform distribution of synthesized nanoparticles. After extensive scanning electron microscopy of multiple samples, it was noticeable that the acetone pretreatment provided more consistent results of homogenous coverage and quality of nanoparticle synthesis.

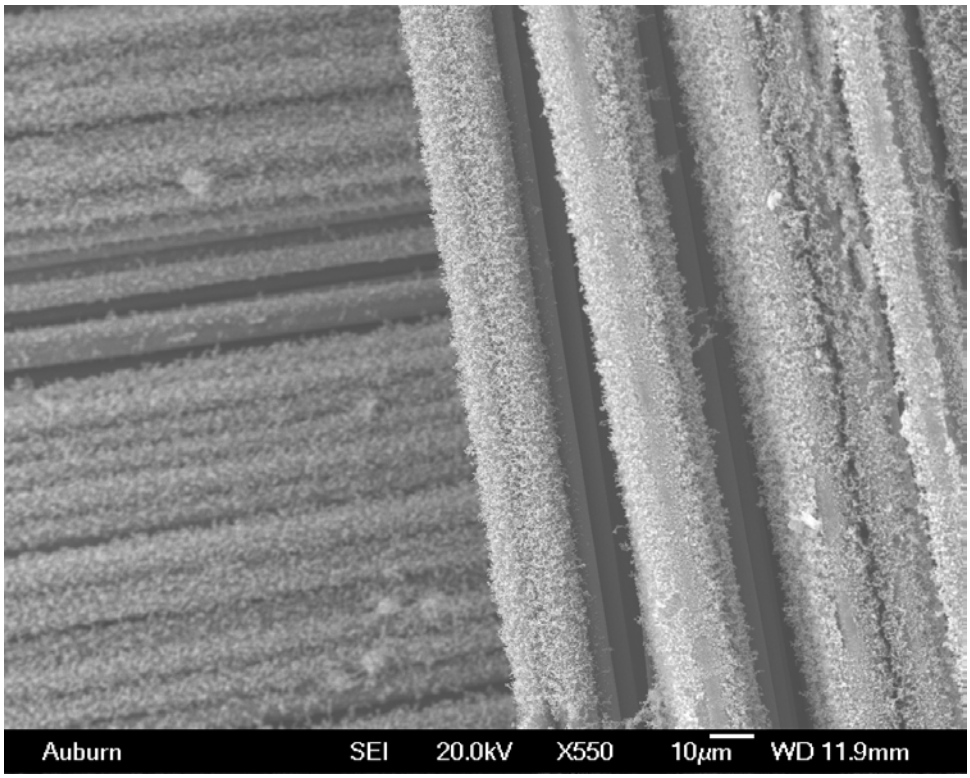

Figure 36: APT Carbon Fiber Fabric after introduction of catalyst and Microwave Irradiation

3.3.5.4 Microwave Treated CF Fabrics with Addition of Carbon Containing Solvents

With the addition of carbon containing solvents, a significant difference in the growth of carbon nanostructures was seen. The solvents that were chosen all contained extra carbon molecules that assisted in improving the synthesis and overall coverage of the carbon nanostructures. In this section, the improvements of carbon nanostructure formation will be reviewed and broken down by the use of each solvent. Acetone pretreated fabrics were chosen based on the superior quality of coverage and density of carbon nanostructures compared to that of fabrics with no pretreatment or microwave pretreatment. In addition, the acetone pretreatment would not lend to significant damage of the carbon fiber as seen in the mechanical studies of the fibers themselves after being subjected to different pretreatments and microwave assisted carbonization.

3.3.5.4.1 Hexane (Hex)

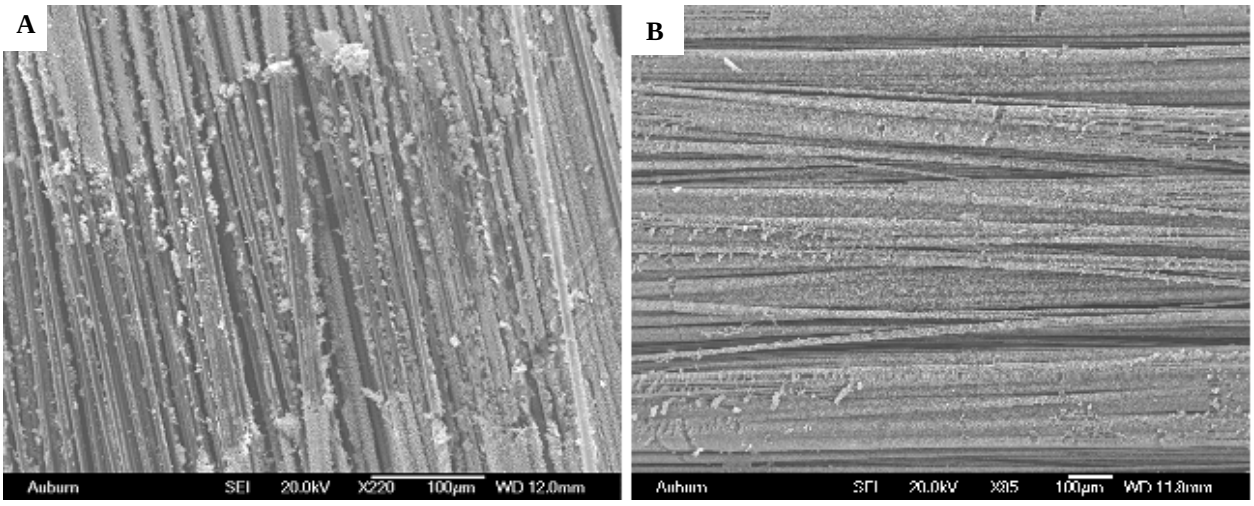

Figure 37: (A) APT CF Fabric without Hexane; (B) APT CF Fabric with Hexane Addition

With the addition of hexane, there was a substantial difference between fabric with and without the solvent. It can be seen in previous sections that acetone pretreated fabrics provide adequate nanoparticle growth and coverage, yet with hexane the coverage and density improved further. In Figure 37, the image on the left presents fabric that is absent of the solvent addition. As a whole, the quality and coverage is sufficient, but upon further inspection, there are sections present that display patchy coverage. This could be due to concentrated amounts of ferrocene in some areas while absent in others. This would make sense due to ferrocene being the major contributor in the nanoparticle synthesis. With hexane present, the image on the right, more carbon molecules are homogenously distributed causing a much more uniform coverage of particles. Ferrocene is the catalyst, yet hexane contains numerous carbon molecules that assist in the formation of carbon nanoparticles.

3.3.5.4.2 Ethanol (EtOH)

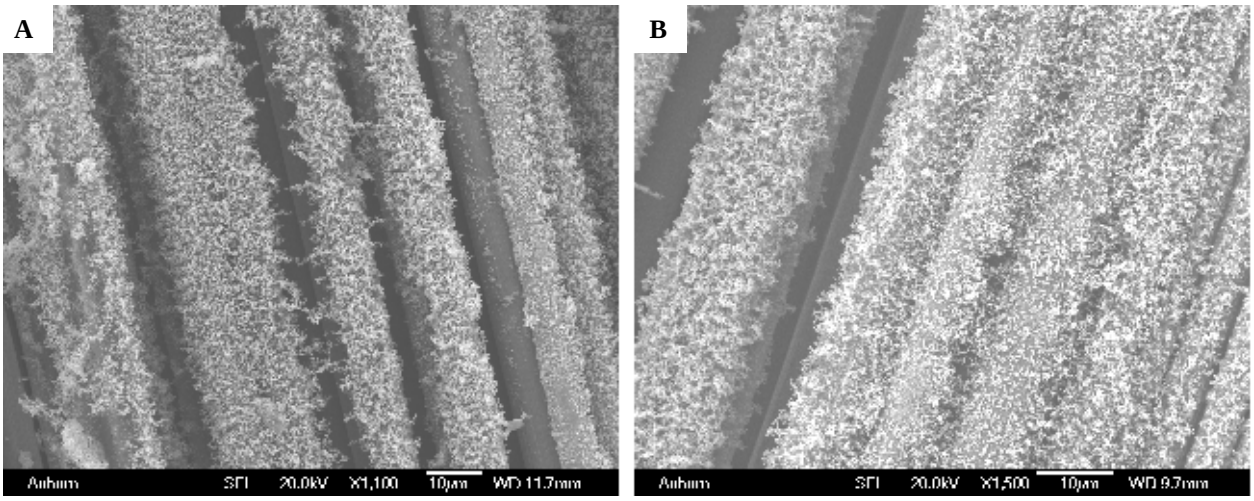

Figure 38: (A) APT CF Fabric without EtOH; (B) APT CF Fabric with EtOH Addition

Ethanol is made up of a linear chain of two carbon molecules with an alcohol molecule attached. It was an interesting case. Being that there were less carbon molecules in the solvent, there was skepticism on whether it would be a useful growth enhancer. Compared to hexane, ethanol only has two carbon molecules in its chain while hexane boasts six. One would think that by this fact alone that hexane would be a significantly better growth enhancer. With that being said, although hexane provided better overall coverage and growth density, ethanol did a sufficient job in improving the coverage and density of carbon nanoparticles compared to a fabric with no solvent addition. This can clearly be seen in Figure 38. Compared to the image on the left, the image on the right has better density and is much more uniform than the aforementioned in areas of extensive growth. Although, the overall coverage of nanoparticles on the fabric did leave something to be desired as it was not far superior to the fabrics with no solvent addition.

3.3.5.4.3 Tetrahydrofuran (THF)

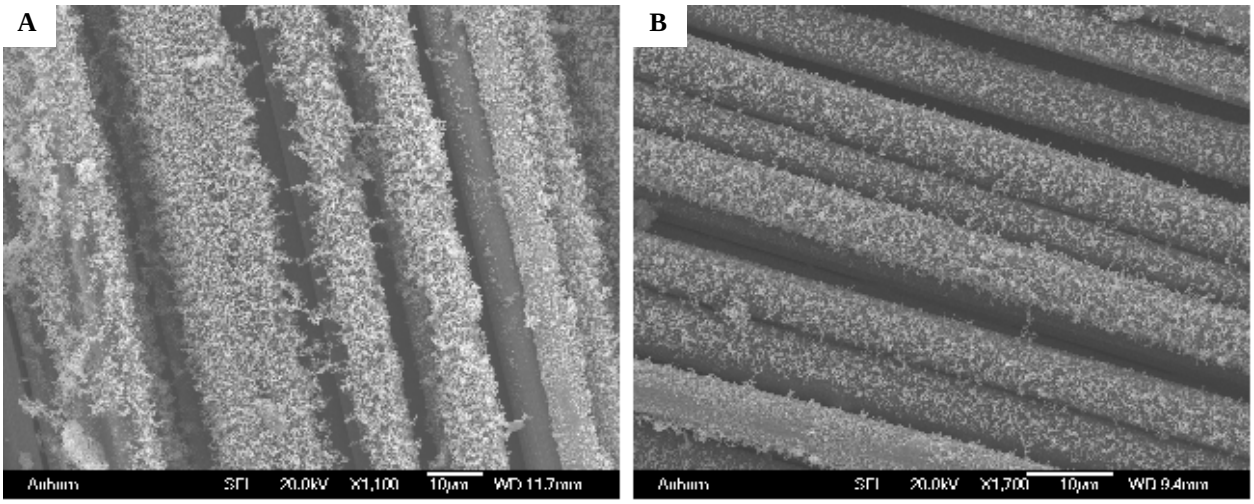

Figure 39: (A) APT CF Fabric without THF; (B) APT CF Fabric with THF Addition

Tetrahydrofuran is a solvent that consists on a five member ring containing four carbon molecules and one oxygen molecule bond by single bonds. This solvent was the only ring structured solvent that was used as a growth enhancer. As can be seen in Figure 39, the addition of THF provided for a uniform growth pattern compared to acetone pretreated fabric with no solvent addition. The density of the nanoparticles was considerably less than fabric with no solvent addition, but does not ensure a negative impact when combined into a composite material. One considerable concern in creating a laminate structure would be how the amount of nanoparticles created would impact the mechanical capability of the final composite. It could be possible for a large amount of carbon nanostructures attached to the surface to hinder the ability of epoxy molecules to bond with the surface of the carbon fiber fabric. If this were to occur, it is foreseen that there would be large voids in the composite which would lead to catastrophic failure. The less dense coverage of particles could be a significant advantage of THF's use in enhancing the quality of the overall composite.

Another advantage that THF was seen to provide was the formation of actual carbon nanotubes on the surface of the fabric. This can be seen in the highly magnified SEM micrograph below.

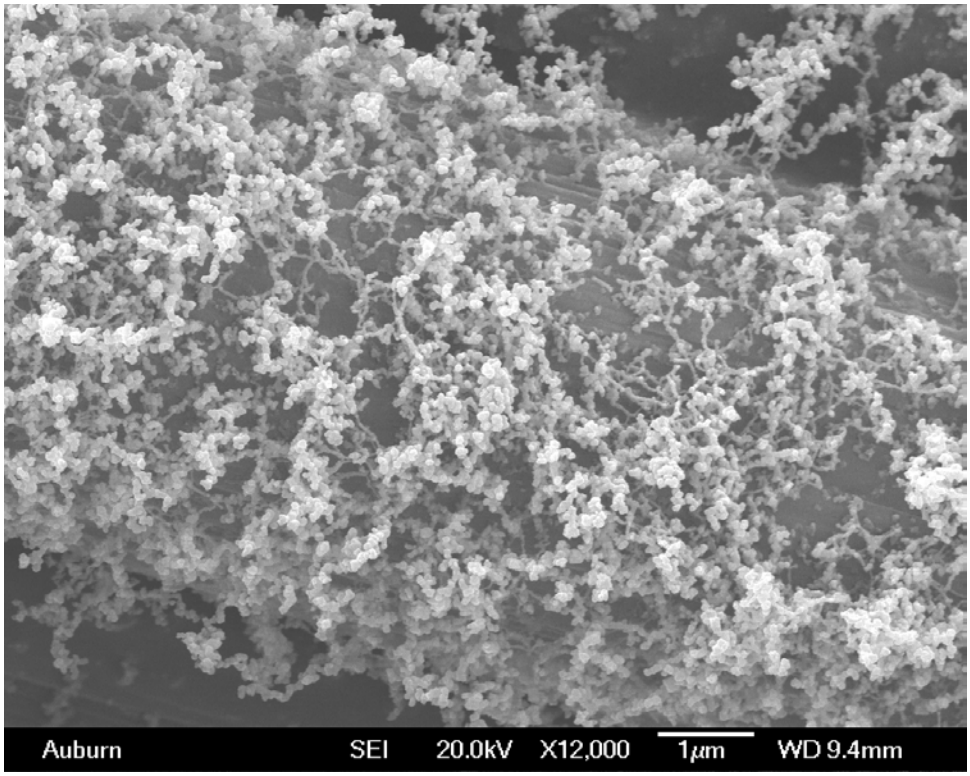

Figure 40: APT Carbon Fiber Fabric with THF Addition displaying CNT Formation

While a majority of the nanostructures created where nanoparticles, THF was the only solvent to produce any CNTs that were visible. Many of the other solvents produce structures that resembled CNTs, but upon further examination, the structures were merely nanoparticles that were touching or potentially bond by van der wall forces.

3.3.6 Tensile Results of Fibers after Different Treatment Methods

An Instron tensile testing machine was used to test single fibers from different treated fabrics. Single fibers were extracted from the treated fabrics and were placed into coupons for

testing. The coupons and the testing parameters corresponded to ASTM standard D3379-75. The results of these tests can be seen below in the following figures.

The virgin carbon fibers produced the highest stress and strain of any of the samples. This is easily explained by not having any treatment of any kind. The epoxy sizing is still present on the surface and helps protect the fiber under the high stresses introduced by tensile testing.

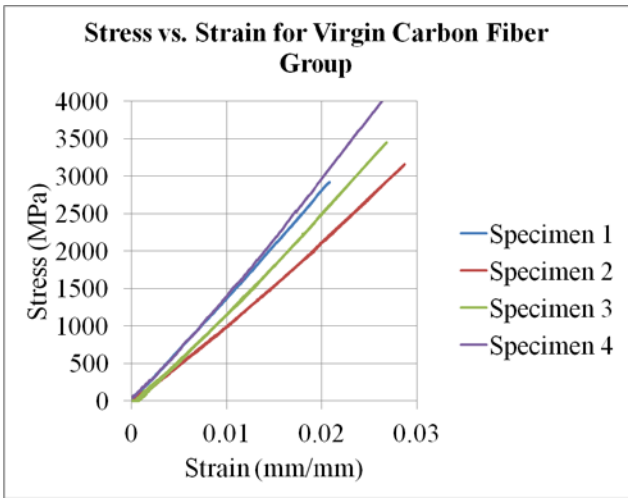

Figure 41: Stress vs. Strain Graph for Virgin Carbon Fiber

Upon pretreatment, the values of stress and strain considerably vary. It can be seen in figure 42 A, that upon microwave pretreatment of 45 sec, the maximum stress and strain were significantly reduced. The maximum stress is reduced by approximately 28%, while the strain the fibers could handle was reduced by approximately 33%. Comparably, the acetone pretreatment was much less damaging to the mechanical strength of the fabric.

When acetone pretreatment was used, the changes in maximum stress were less considerable. The stress was reduced by 14%. While that is still a considerable reduction in strength, it was much less than the microwave pretreated carbon fiber sample. The strain was a comparable value, but was to be expected since the removing of sizing creates a much more

brittle fabric. The addition of ferrocene and microwave irradiation was also observed for their effect on the strength of the fabric after carbon nanoparticle syntheisis.

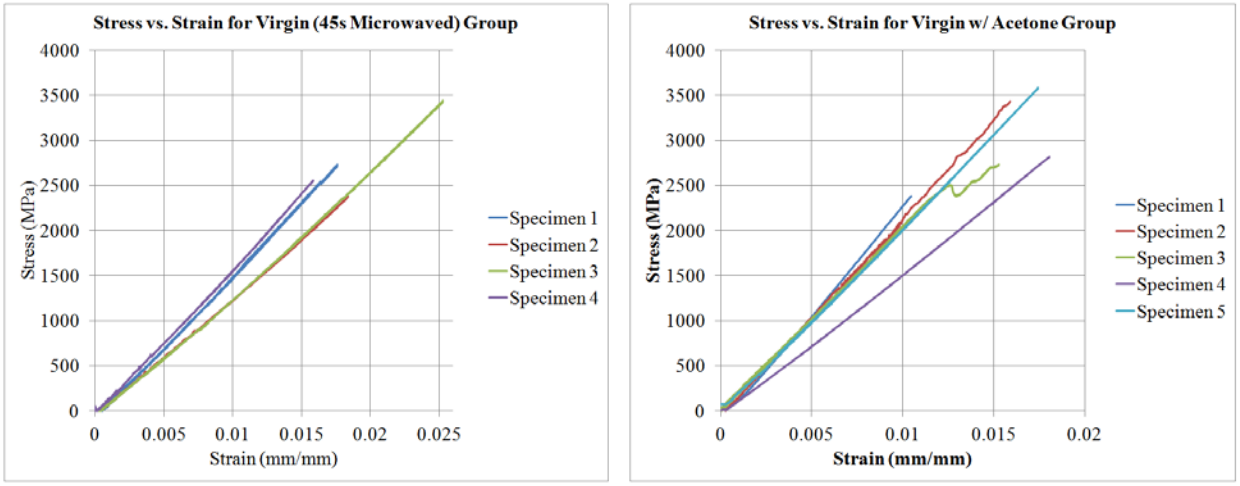

Figure 42: Stress vs. Strain Graphs, A.)MPT CF Fabric; B.) APT CF Fabric

The catalyst addition and microwave irradiation did not claim a major change in the stress and strain compared to the pretreated fabrics. This was encouraging because nanostructures could be synthesized on the surface of the fabrics without compromising any additional strength of the fibers.

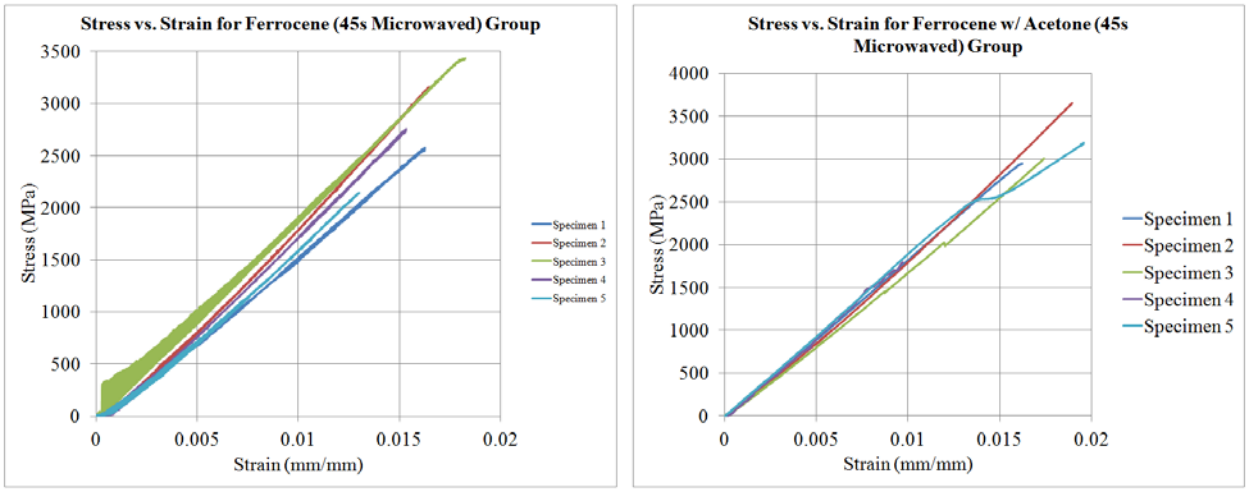

Figure 43: Stress vs. Strain Graphs, A.)MPT CF Fabric with Ferrocene; B.) APT CF Fabric with Ferrocene

A summary of the results from tensile testing, using different pretreatment methods and synthesis processes, can be seen in Table 2. Table 3provides the data from Table 2 as a percentage of the as-received carbon fiber fabric values for a better understanding.

Table 2: Summary of Single Fiber Tensile Testing

Specimen		Breaking Load (N)	Strength (Mpa)	Modulus (Gpa)	Axial Failure Strain (mm/mm)
Virgin	Mean	0.0805	3425.42	131.43	0.0259
	Standard Deviation	0.0125	533.58	19.74	0.0035
	Standard Deviation (%)	15.58	15.58	15.02	13.42
Microwaved	Mean	0.0652	2774.18	144.96	0.0193
	Standard Deviation	0.0109	463.62	16.19	0.0041
	Standard Deviation (%)	16.71	16.71	11.17	21.47
Ferrocene (45s Microwaved)	Mean	0.0661	2811.49	176.28	0.0159
	Standard Deviation	0.0118	503.37	14.61	0.0019
	Standard Deviation (%)	17.90	17.90	8.29	12.04
Virgin w/ Acetone	Mean	0.0667	2985.93	201.45	0.0154
	Standard Deviation	0.0103	503.46	27.40	0.0030
	Standard Deviation (%)	15.41	16.86	13.60	19.41
Virgin w/ Acetone (15s Microwaved)	Mean	0.0860	3564.07	191.66	0.0202
	Standard Deviation	0.0112	364.03	17.59	0.0030
	Standard Deviation (%)	13.02	10.21	9.18	14.98
Virgin w/ Acetone (30s Microwaved)	Mean	0.0712	3030.49	190.48	0.0159
	Standard Deviation	0.0183	778.06	20.83	0.0039
	Standard Deviation (%)	25.67	25.67	10.93	24.25
Virgin w/ Acetone (45s Microwaved)	Mean	0.0571	2430.49	190.72	0.0130
	Standard Deviation	0.0156	664.11	11.67	0.0041
	Standard Deviation (%)	27.32	27.32	6.12	31.44
Ferrocene w/ Acetone (15s Microwaved)	Mean	0.0738	3140.59	195.33	0.0169
	Standard Deviation	0.0117	499.16	11.53	0.0033
	Standard Deviation (%)	15.89	15.89	5.90	19.26
Ferrocene w/ Acetone (30s Microwaved)	Mean	0.0649	2761.86	192.03	0.0144
	Standard Deviation	0.0096	409.21	21.74	0.0016
	Standard Deviation (%)	14.82	14.82	11.32	11.37
Ferrocene w/ Acetone (45s Microwaved)	Mean	0.0691	2940.46	185.49	0.0164
	Standard Deviation	0.0151	643.20	10.98	0.0039
	Standard Deviation (%)	21.87	21.87	5.92	24.10

Table 3: Comparison of Tensile Results as Percentage of As-Received Fabric Values

Specimen	Mean Breaking Load	Mean Tensile Strength	Mean Young's Modulus	Mean Axial Failure Strain
Virgin	100.00	100.00	100.00	100.00
Microwaved	80.99	80.99	110.29	74.35
Ferrocene (45s Microwaved)	82.08	82.08	134.12	61.26
Virgin w/ Acetone	82.84	87.17	153.27	59.50
Virgin w/ Acetone (15s Microwaved)	106.80	104.05	145.82	77.83
Virgin w/ Acetone (30s Microwaved)	88.47	88.47	144.92	61.43
Virgin w/ Acetone (45s Microwaved)	70.95	70.95	145.11	50.16
Ferrocene w/ Acetone (15s Microwaved)	91.69	91.69	148.62	65.20
Ferrocene w/ Acetone (30s Microwaved)	80.63	80.63	146.11	55.53
Ferrocene w/ Acetone (45s Microwaved)	85.84	85.84	141.13	63.13

3.3.7 Thermogravimetric Analysis of Synthesized Fillers and Epoxy-Filler Composites

TGA was used to characterize the fillers and the epoxy-filler composites for their thermal stability. The major degradations of the samples were shown and the weight percentages lost as well as retained are important characteristics to discuss.

3.3.7.1 PPy Morphologies

It can be seen in figure 44 that the morphologies that were polymerized in the presence of HCl have less interaction with the air that is present within the furnace. PPy fiber (PPyF) polymerized in HCl retains the most weight percentage, approximately 10%, compared to the PPy granule samples (PPyG) and is the only sample that is not completely decomposed. It is worth noting that all samples have the approximately the same major degradation temperature between 250-275˚C.

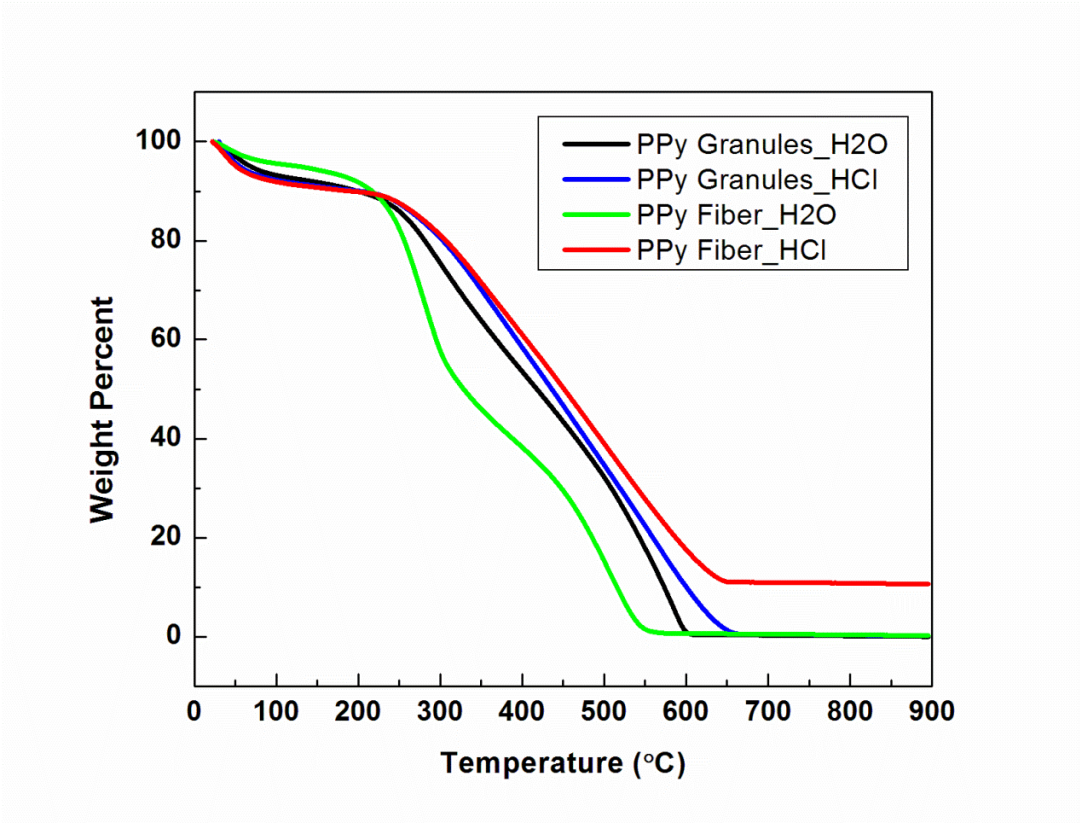

Figure 44: TGA Analysis of different PPy Morphologies

3.3.7.2 Milled Carbon Fiber Substrate Samples

The synthesized milled carbon fiber samples were also analyzed for their thermal stability. The goal was to compare the PPy-MCF composites to those samples that underwent

MIC. In the previous SEM micrographs, CNT synthesis was confirmed and TGA analysis was completed to determine their effect on the samples thermal properties.

In Figure 45, the PPyG-MCF composites were compared to the MIC counterparts. It can be seen that the PPyG-MCF samples have two major degradation temperatures when polymerized in both water and HCl. The first occurs around 300˚C and results in a 20-30% weight loss. This range of weight loss can be expressed at the conducting polymer portion of the composite as it is typically about 30% of the total weight of the sample and has a much lower degradation temperature. The second takes place at approximately 650˚C and results in the complete decomposition of the sample. This weight loss can be attributed to the decomposition of MCF.

For the samples that underwent MIC and produced CNT growth, only one major degradation temperature is present. It occurs at approximately 450˚C. This is important to note since epoxy claims a degradation temperature of 400-450˚C. This should ensure that the filler will not begin to decompose until the epoxy itself begins to. The effect of the filler on the composite's overall thermal stability will be examined in the following sections.

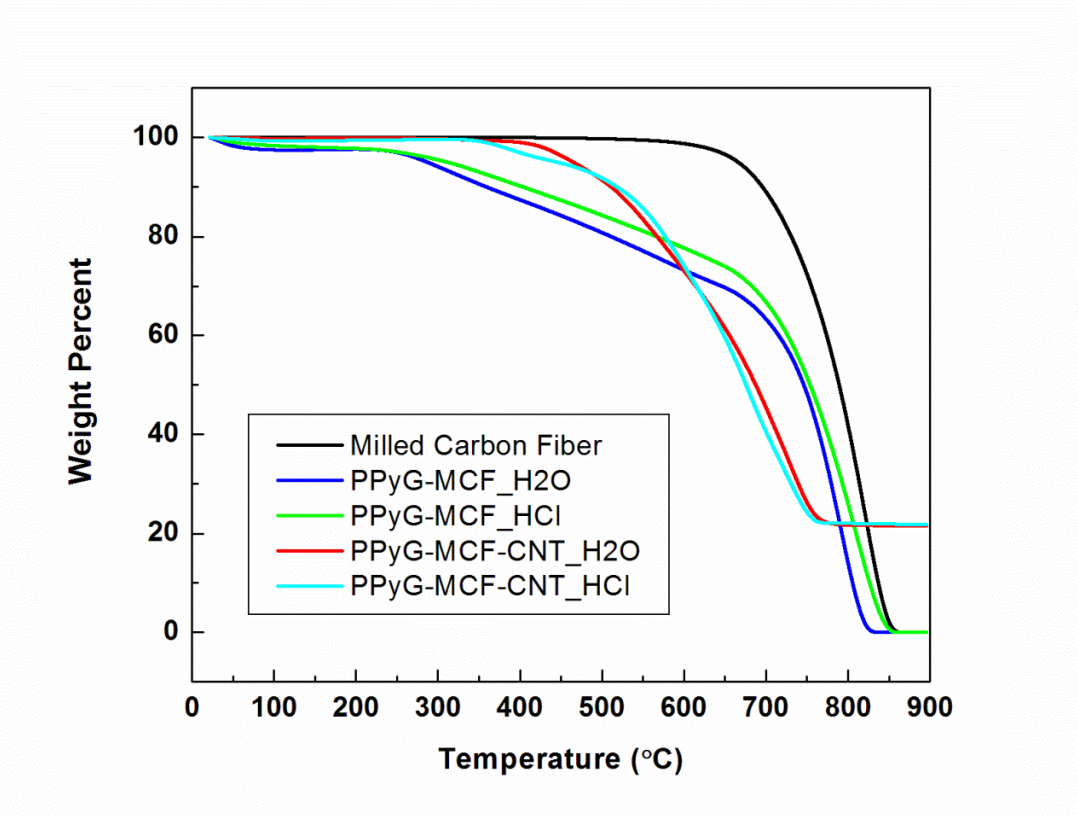

Figure 45: TGA Analysis of Synthesized PPyG-Milled Carbon Fiber and MIC Substrates

For the PPyF-MCF composite samples, a similar phenomenon took place. There were two major degradation temperatures present, the second which was higher than that of the PPyG-MCF composites. The first major degradation temperature took place at approximately 300˚C. For the DI water sample, the second degradation took place at 550˚C while the HCl sample's occurred at 650˚C. Similarly, both PPyF-MCF composites were fully decomposed. The samples that underwent MIC had two major degradation ranges. The first began at approximately 350˚C and resulted in a weight loss of roughly 20%. The second range began around 550˚C and ended just after 750˚C. The weight loss during this range was 60 and 70% in DI water and HCl, respectively.

Due a lack of significant difference in the PPyG-MCF-CNT samples compared to that of PPyF-MCF-CNT and PPyF-MCF's superior CNT growth, PPyF-MCF-CNT that was

polymerized in HCl was chosen as the filler to be introduced into the epoxy system. Like previously stated, the filler weight ratio was chosen as 3% weight to allow for enough filler to initiate an improvement in mechanical properties and also maximize potential electrical conductivity.

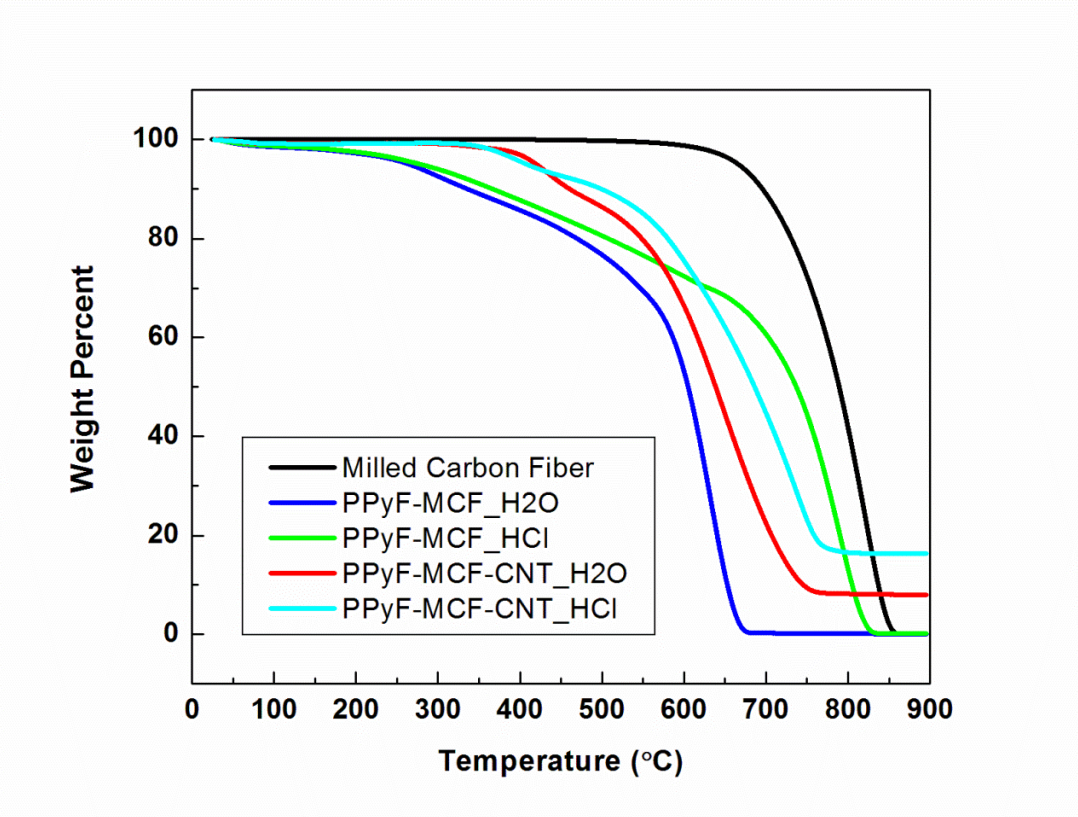

Figure 46: TGA Analysis of Synthesized PPyF-Milled Carbon Fiber and MIC Substrates

3.3.7.3 Epoxy-MCF filler Composites

For the epoxy composites, neat Epon, MCF-Epon, and PPyF-MCF-CNT-Epon were cast in order to understand the fillers effect on the overall composite. For neat Epon, the composite went through two-step decomposition and was initially thermally stable up to 350˚C. Between 350 and 450˚C, a major degradation was observed. This degradation resulted in a weight loss of approximately 60%. After 450˚C, the composite went through a more gradual decomposition resulting in approx. 10% weight loss. At just above 500°C, the sample goes through another

large decomposition step in which the remainder of the weight of the sample is burned completely. This last decomposition step ended around 650°C and resulted in 30% weight loss.

Upon the addition of 3% by weight of milled carbon fiber, negligible changes can be seen. The sample decomposes at the same temperature ranges and goes through a similar two-step decomposition as the neat epon sample. The slight changes in the total weight loss, in both stages, can be attributed to the presence of MCF.

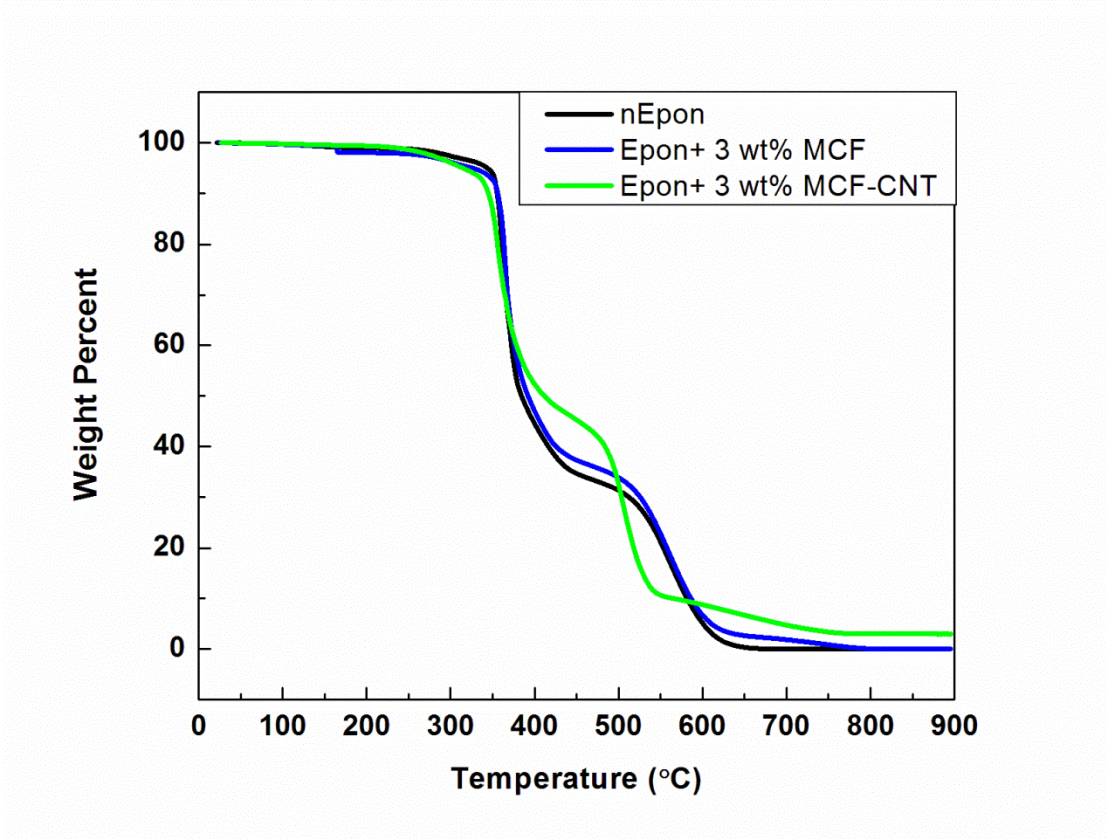

Figure 47: TGA Analysis of neat Epon and Filler-Epon Composites

3.3.7.4 Carbon Fiber Fabric Substrate Samples

For the second substrate that was used, carbon fiber fabric, TGA analysis was completed to understand the effect of pretreatment and MIC on the major strength contributor of a potential carbon fabric laminate composite. CFF with no pretreatment, acetone pretreated CFF, and

acetone pretreated CFF with the addition of THF after MIC were all subjected to TGA experiments with a temperature range of 0-900˚C.

All fabric samples had a major decomposition of approximately 650˚C. Each sample completely decomposed, but that occurred at slightly different temperatures. As-received CFF completely decomposed by 850˚C, while AT CFF and MW AT CFF with THF completely decomposed by approx. 835 and 825˚C, respectively. This difference could be considered negligible.

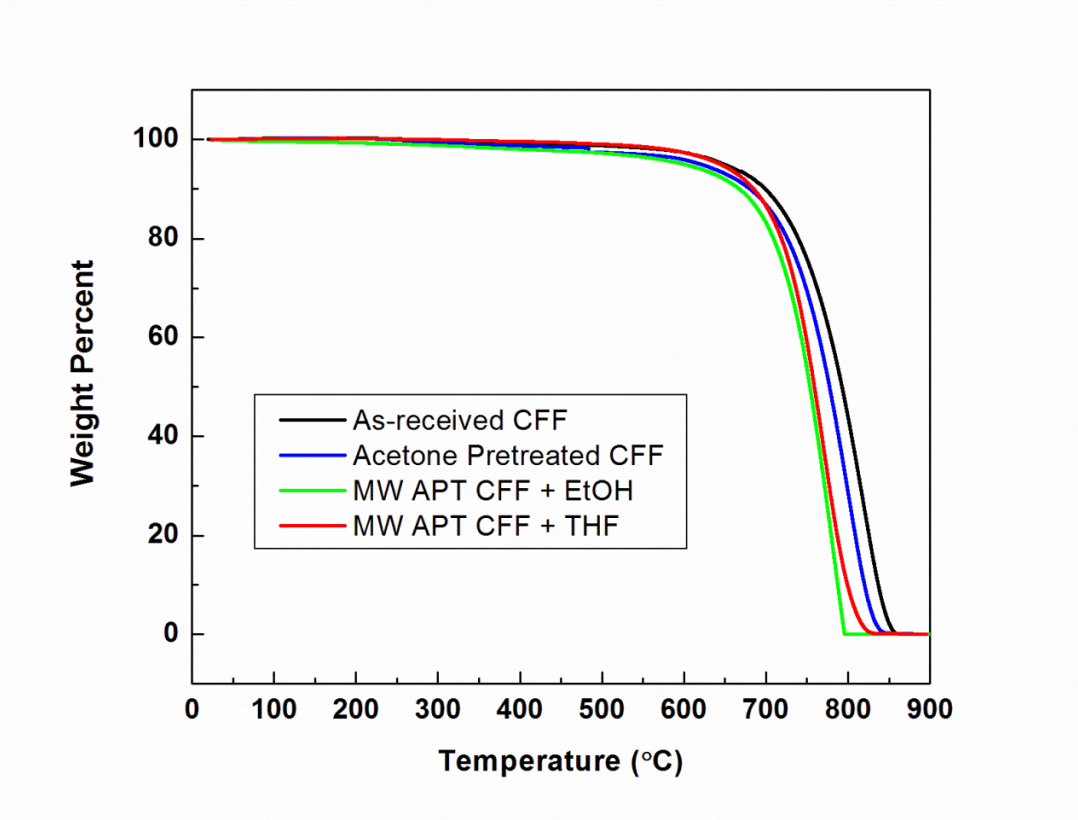

Figure 48: TGA Analysis of Carbon Fiber Fabric with and without MIC

3.3.8 Differential Scanning Calorimetry of Filler-Epoxy Composites

DSC was used to run heat/cool/heat experiments on neat epon and epon-filler composites and can be seen in Figure 49. This was done to characterize the material before and after maximized percent of curing to understand the fillers effects on the glass transition and the fillers

participation on the curing of the composite samples. Neat epon starts with a large absorption of heat just before its initial glass transition. After the glass transition (which was also confirmed by DMA), it was seen that the sample began to cure around 100-125°C. This can be determined by the exothermic release of heat designated by the upward (exo) pointing curve. After the sample is cooled, it was seen that the T_g had shifted toward a higher temperature and the curing curve was absent. This was a universal trend throughout all the samples.

The main difference that was seen was that the area under the exothermic curves of the samples containing filler was much larger than that of neat epon. In the samples containing filler, the area under this exothermic curve was much larger/than that of neat epoxy. From this curve, it can be determined how much of the sample was crosslinked. Therefore, the samples were not cured to their full potential, and contained less crosslinking than neat epon.

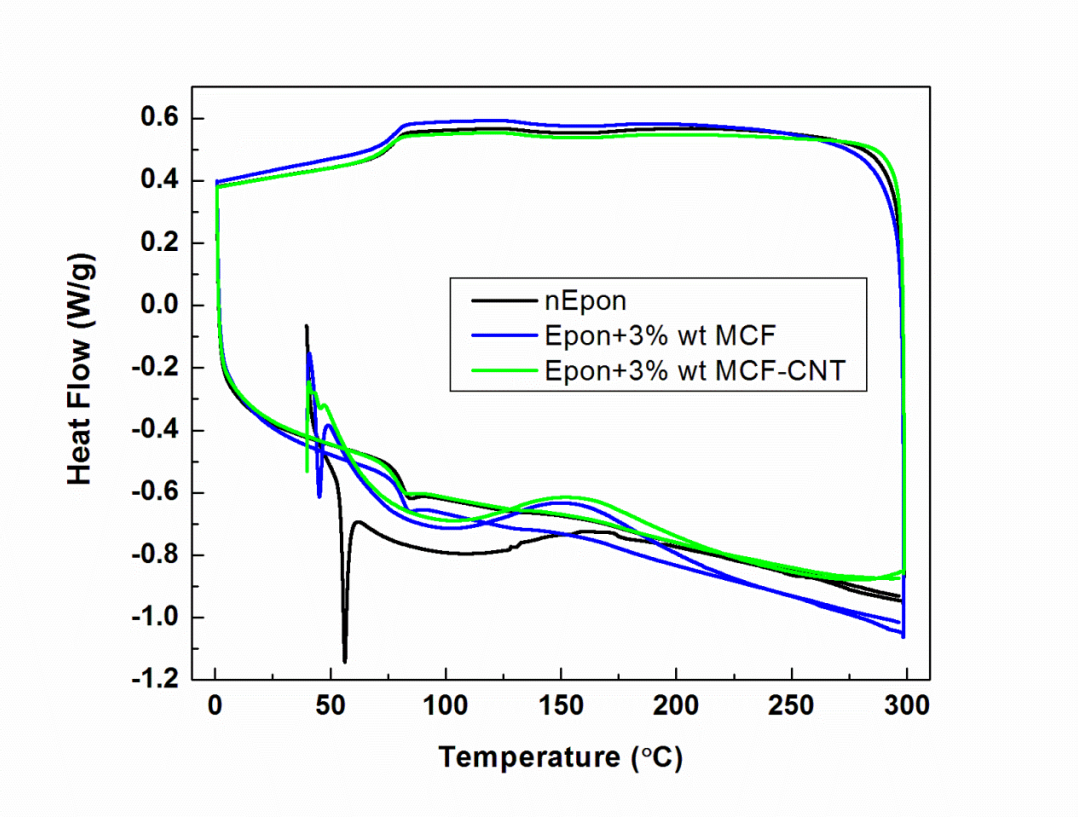

Figure 49: DSC Analysis of neat Epon and Filler-Epon Composites

3.3.9 Dynamic Mechanical Analysis of Filler-Epoxy Composites

The samples cast using epon and the milled carbon fiber substrates were machined to an appropriate size and subjected to 3 pt. bending DMA experiments. DMA experiments return vital information, including storage (E') and loss (E") moduli as well as a tan delta curve that correlates to the glass transition temperature (T_g). For these experiments, the apparatus that was used had a span length of 10 mm. Taking this into consideration, the samples were machined to have a thickness of less than 1.5 mm.

Below in Table 3, data from DMA testing as well as the calculations for crosslink density can be seen. The glass transition temperature was taken as the peak of the tan delta curve provided from testing. In order to calculate the crosslinking density, the following equation was used, $E' = 3nRT$ where n is the crosslink density and R is universal gas constant.[20,21] E' correlates to the storage modulus 20°C above the T_g, while T is the temperature at this E'.

Table 4: DMA Data and Calculated Crosslink Density

	T_g (°C)	T_g+20 (°C)	E' at 20°C above T_g (Pa)	Crosslink Density, n (mol/m^3)	Fracture Toughness
nEpon	59.6	79.6	9.15×10^6	1040	1.3 $MPa/m^{0.5}$
Epon + 3wt % MCF	54.6	74.6	4.25×10^6	490	1.84 $MPa/m^{0.5}$
Epon + 3wt % MCF-CNT	51.5	71.5	4.93×10^6	573	1.58 $MPa/m^{0.5}$

The crosslink density in the samples that contained filler was almost half the value of the neat Epon samples. This was an interesting point. This would lead one to believe that the added filler is in some fashion hindering the amount of crosslinking in the sample. Based on some preliminary results, it is shown to be true. Since more crosslinking typically leads to a more brittle response, the samples that had lower crosslinking showed higher fracture toughness in preliminary fracture toughness experiments. This can be confirmed by the data shown in Table 3.

3.3.10 Electrical Conductivity Studies

3.3.10.1 PPy-Milled Carbon Fiber-Epoxy Composite

Four probe conductivity measurements were taken of MCF Epoxy composite and PPy-MCF Epoxy composites with 3% weight of filler using a Keithley 4200 measurement system. Measurements of the composite had to be taken due to the difficulty and unreliability of pressing the pure filler using a Teflon mold. The epoxy composites were cut into rectangular test samples with the following dimensions: 40mm x 9.5mm x 2mm. A neat epoxy sample was also tested as a control. The four probe measurement resulted in giving no resistance measurement. The machine's capable range reaches a resistance of TΩ. That being said, the resistance of the samples had to exceed the capable range of the equipment used. All samples went through the same process and returned the same results. In this case, the resistance is not known for sure. An estimation of resistivity can be estimated using the following equation.

$$\rho = 2\pi * s * F * V/I$$

The probe spacing (1mm) is provided by s. F is correction factor; in this case it is 1. The measured resistance is V/I and resistivity is represented by ρ. Based on calibrating with a known sample, it was determined that the equipment could measure a sample whose measured resistance was below 10 GΩ. Therefore, the resistivity was calculated as seen below.

$$\rho = 2\pi * s * F * 10\ G\Omega$$

This estimation resulted in a resistivity that was greater than 6.28×10^7 Ω*m. All the samples were calculated to be the same, therefore the true resistivity is not known. This could be explained by the amount of filler present. Since the weight percent of filler was only 3% and carbon fiber is known to be conductive, it was determined that the percolation threshold was not

reached. This means that there was not enough filler to create a network for electrons to travel through and the insulating epoxy hindered transport between the filler links.

3.3.10.2 Carbon Fabric Filler

The resistivity results of the 2 probe volt meter testing can be seen below in Table 3. The electrical conductivity was calculated using the following equation [21].

$$\sigma = \frac{l}{R \times A}$$

The length is defined by, l. R is the resistivity while, A, is the cross sectional area.

The as-received fabric had an average resistance of 43.24 ohms. The epoxy sizing could affect the resistance since epoxy tends to be insulating. Therefore, acetone pretreated fabric was tested to compare. The APT carbon fiber fabric actually produced a slightly higher resistance than the as-received sample. This can be explained by the difficulty of placing the probes on the fabric without the fiber moving from under the probe tips. Since the best results would be measured if the tips were touching the same fibers as the other probe, the resistance that was measured was higher due to the difficult of the fiber within the fabric staying in place. Upon microwave irradiation and carbon nanostructure synthesis, the resistivity is reduced by at least 4 times that of the as-received sample. This translates to an increase of 7 times the conductivity of the as-received carbon fiber fabric. The previous SEM micrographs are extremely useful when understanding why the addition of ethanol enhanced the electrical conductivity. When viewing the images, it can clearly be seen that most of the surfaces are covered by a dense nanoparticle forest that is well connected. The THF sample has a less dense network and has gaps in the coverage on the surface of the fibers. Therefore, the difference in conductivity can be attributed to the enhanced coverage in the ethanol sample even though no CNTs can be seen.

Table 4: Resistance and Calculated Electrical Conductivity of Carbon Fabric Samples

	Resistance (Ohms)	**Electrical Conductivity (S/cm)**
As-Received Carbon Fiber Fabric	43.24	6.93
Acetone Treated CFF	45.31	7.98
Acetone Treated CFF + THF	11.98	33.52
Acetone Treated CFF + EtOH	7.71	52.30

CHAPTER 4

CONCLUSIONS AND THE FUTURE WORK

4.1 Conclusions

In conclusion, multi-dimensional nano-conductors were synthesized using a microwave assisted carbonization technique with two different carbon substrates; i.) Milled Carbon Fiber, ii.) Carbon Fiber Fabric. Milled carbon fiber was subjected to an in-situ polymerization of polypyrrole nanostructures in two different aqueous systems: DI water and 1M Hydrochloric Acid. Afterward, the PPy-MCF composites were dry mixed with ferrocene, a metallocene catalyst, in a 1:1 ratio and subjected to microwave irradiation. The carbon fiber fabric underwent a liquid metallocene catalyst soaking by dissolving ferrocene in Toluene. After sufficient drying, the fabrics were also subjected to microwave irradiation. After treatment and carbon nanostructure growth, the synthesized fillers, fabrics, and corresponding epoxy composites were characterized using Scanning Electron Microscopy, Tensile Testing, Thermogravimetric Analysis, Differential Scanning Calorimetry, Dynamic Mechanical Analysis, and electrical conductivity measurements.

The results of the forementioned testing demonstrated the best synthesized material from each substrate. For the MCF substrate, the PPy fiber-MCF-CNT sample that was from the HCl system proved to be the most thermally stable while producing the best CNT growth, coverage, and quality. For the carbon fabric substrate, the acetone pretreated fabric with the ethanol

addition proved to maintain a sufficient thermal stability while providing the best electrical conductivity.

Upon characterizing the final epoxy composites by DSC and DMA, it was learned that the filler was hindering the composite's ability to maximize the amount of crosslinks within the sample which could lead to increased ductility or potential mechanical failure.

This work provides pertinent information for using this microwave assisted carbonization on carbon substrates to be used as fillers in epoxy composites. The synthesized fillers provided a cheaper alternative to what is currently available on the market and provided specific enhancements that would lend usefulness to structural applications in the construction and aerospace industries. Yet, although enhancements in some properties were seen, the composites need to be further characterized to completely understand the fillers effect on the curing of the composite.

4.2 Recommended Future Work

In the future, MCF will be subjected to the same liquid metallocene catalyst treatment that the carbon fiber fabric underwent. This will be executed as an attempt to improve the surface interaction between the MCF and as-grown CNTs and remove the need of conducting polymer presence.

For determination of electrical capabilities, larger weight percentages of the PPy-MCF samples after microwave irradiation will be incorporated into the epoxy to find the percolation threshold.

In addition, the synthesized fabric samples will be incorporated into laminate composites using Epoxy and PBO resins and tested for their electrical and mechanical properties, such as 3 point bending breaking strength and the interlaminar shear strength.

References

1. Kopeliovich, Dmitri. "Classification of Composites." *SubsTech, Substances and Technologies*. Web. 06 Jan. 2014. <http://www.substech.com/dokuwiki/doku.php?id=classification_of_composites>.
2. *Introduction to Composite Materials*. ASM International, 2012. Print. <http://asminternational.org/content/ASM/StoreFiles/05287G_Sample_Chapter.pdf>.
3. "Introduction to Composite Materials." *EFunda*. N.p., n.d. Web. 07 Jan. 2014. <http://www.efunda.com/formulae/solid_mechanics/composites/comp_intro.cfm>.
4. "Silcon Aluminum." *SP3 Diamond Cutting Tools*. 2014. Web. 7 Jan. 2014. <http://sp3cuttingtools.com/applications/silicon-aluminum.html>.
5. "Composite Materials for Future Cities." *City Composites*. N.p., 2012. Web. 7 Jan. 2014. <http://www.citycomposites.com/manhole-covers/>.
6. Eastman, Michael. "Structural Composite Materials." *Materials World Modules*. The University of Texas at El Paso, 2010. Web. 8 Jan. 2014. <http://materialsworld.utep.edu/Modules/Composite/Composite%20Materials/composite%20materials.htm>.
7. Ashby, M. F., and David R. H. Jones. "Chapter 25 - Composites: Fibrous, Particulate and Foamed." *Engineering Materials 2: An Introduction to Microstructures, Processing, and Design*. Oxford: Pergamon, 1986. 263-75. Print.

8. "Home Made Composites - Composites in Daily Life." *Home Made Composites (HomMaCom)*. Web. 09 Jan. 2014. <http://www.composites.ugent.be/home_made_composites/composites_in_daily_life.html>.
9. "Carbon Nanotubes." *Cnanotech.com*. 2014. Web. 9 Jan. 2014. <http://www.cnanotech.com/2012/08/07/history-of-carbon-nanotubes.html>.
10. "Carbon Nanotubes." *The Role of Chemistry in History*. N.p., 24 Apr. 2008. Web. 10 Jan. 2014. <http://itech.dickinson.edu/chemistry/?p=423>.
11. "Synthesis of Acetylferrocene." *Laboratory Reference Manual*. Reed College, Web. 10 Jan. 2014. <http://academic.reed.edu/chemistry/alan/201_202/lab_manual/Expt_ferrocene/background.html>.
12. Vernitskaya, Tat'yana V., and Oleg N. Efimov. "Polypyrrole: A Conducting Polymer; Its Synthesis, Properties and Applications." *Russian Chemical Reviews* 66.5 (1997): 443-57. Print.
13. Steinke. "Conducting Polymers." *Department of Chemistry*. Imperial College London, Web. 11 Jan. 2014. <http://www3.imperial.ac.uk/ugprospectus/facultiesanddepartments/chemistry>.
14. Lai, E. K. W. Conducting polymer composite films for the electrocatalytic reduction of oxygen, Thesis, 1994, Simon Fraser University, British Columbia, Canada
15. Zhang, X. PFEN 7970 Conductive polymer materials - Lecture 1 **2013**, Auburn University, Auburn, Alabama

16. Zhang, X. PFEN 7970 Conductive polymer materials - Lecture 4 2013, Auburn University, Auburn, Alabama
17. Anderson, C; Davidson, E. “Conducting Polymers.” Physics 141A – Introduction to Solid-State Physics. April 2013. < http://budker.berkeley.edu/Physics141_2013>.
18. Zhang, X.; Manohar, S. K. *J. Am. Chem. Soc.* 2005, 127, 14156-14157
19. Jin, Xin, Wenyu Wang, Lina Bian, Changfa Xiao, Guo Zheng, and Cun Zhou. "The Effect of Polypyrrole Coatings on the Adhesion and Structure Properties of UHMWPE Fiber." *Synthetic Metals* 161.11-12 (June 2011): 984-89. Web. 14 Jan. 2014. <19. http://www.sciencedirect.com/science/article/pii/S0379677911000907>.
20. Liu, Zhen; Wang, Jialai; Kushvaha, Vinod; Poyraz, Selcuk; Tippur, Hareesh; Park, Seongyong; Kim, Moon; Liu, Yang; Bar, Johannes; Chen, Hang and Zhang, Xinyu. *Poptube Approach for Ultrafast Carbon Nanotube Growth*, Chemical Communications, 2011, 47, 9912-9914.
21. L. W. Hill, *Paint and Coating Testing Manual*, J. V. Koleske Ed., Fourteenth Ed. Gardner-Sward Handbook, ASTM, Philadelphia, PA, 1995; Ch. 46, p. 534.
22. L. E. Nielsen, *J. Macromol. Sci-Revs. Macromol. Chem*., C3, 69, 1969.